Linear Acceleration Is a Primary Risk Factor for Concussion and a Target for Prevention

Jessica A. Towns[1]*, Nicholas J. Cecchi[1,2], James W. Hickey[3], William T. O'Brien[3], Spencer S.H. Roberts[4], N. Stewart Pritchard[5,6], Jillian E. Urban[5,6], Joel D. Stitzel[5,6], Gerald A. Grant[7], Michael M. Zeineh[8], Stuart J. McDonald[3,9], David B. Camarillo[1,2]

[1]Department of Bioengineering, Stanford University, Stanford, 94305, USA

*Corresponding author. Email: jtowns03@stanford.edu

[2]SoftShox, Vienna, VA, USA

[3]Department of Neuroscience, School of Translational Medicine, Monash University, Melbourne, 3800, Australia

[4]Centre for Sport Research, Institute for Physical Activity and Nutrition, Deakin University, Geelong, 3220, Australia

[5]Center for Injury Biomechanics, Virginia Tech-Wake Forest University, Winston-Salem, 27101, USA

[6]Wake Forest University School of Medicine, Winston-Salem, 27106, USA

[7]Department of Neurosurgery, Duke University, Durham, 27708, USA

[8]Department of Radiology, Stanford University, Stanford, 94305, USA

[9]Department of Neurology, Alfred Health, Melbourne, 3004, Australia

Abstract:

Head impacts can cause concussion, but the precise biomechanical conditions that produce injury remain uncertain. Rotational acceleration has long been posited as the primary cause and has guided concussion prevention strategies. Using instrumented mouthguards to record head kinematics of diagnosed concussions, we directly tested this hypothesis and found that linear acceleration predicted injury with greater precision than rotational acceleration, while rotational velocity provided additional predictive value. Injury risk functions derived from these measurements indicated substantial predicted concussion risk during typical impacts to an American football helmet. Introducing a liquid-filled helmet pad designed to attenuate linear acceleration reduced predicted risk by up to 52%. These results indicate that effective concussion prevention requires targeting linear acceleration.

Introduction

Traumatic brain injury (TBI) is the second most common neurological disorder in the United States,[1] with an estimated global incidence of nearly 69 million cases per year.[2] While approximately 80−90% of TBIs are concussions, which are classified as "mild" (mTBI),[3] this designation substantially understates the human toll. Most individuals recover within weeks, however, 15-25% of people with an mTBI may have persistent post-concussive symptoms 1 year after the injury, including deficits in attention, memory, and executive function.[4–7] In addition, concussion is associated with psychiatric comorbidities such as depression, emotional dysregulation, and post-traumatic stress disorder, which may persist for years and significantly impair quality of life.[8–11] Despite these co-morbidities and the high prevalence of mTBI, protective technologies such as helmets, vehicles, and playground surfaces are primarily designed and tested to prevent severe TBI, not concussion. Rates of severe TBI have been reduced because the biomechanical causes are better known than those of mTBI.[12,13] Therefore, concussions that frequently occur in transportation, military, sports/recreation, and industrial workplace settings may be preventable with a more precise understanding of the biomechanics from single, isolated impacts.

The biomechanical cause of closed-head TBI was first proposed during World War II, when A.H.S. Holbourn hypothesized that rotational acceleration of the head induces large shear strains within brain tissue, whereas linear acceleration does not.[14] The biophysical basis for the rotational acceleration hypothesis is that the massive human brain is a soft, gel-like structure that shears as it lags behind the rotating skull.[15] In contrast to rotational motion, linear acceleration primarily transmits compressive forces to the head rather than shear. Because the brain and cerebrospinal fluid are nearly incompressible, compressive or tensile loading causes little deformation but can result in large pressures. As a result, rotational head kinematics and brain strain have become the primary diffuse brain injury criteria for many concussion safety testing methodologies.

Early support for the rotational hypothesis emerged from large animal models of moderate-to-severe TBI, and later shifted toward mTBI, or concussion. During the 1960s and 70s, Ommaya and Gennarelli demonstrated that rotational loading could produce loss of consciousness and widespread axonal pathology in non-human primates.[16–18] Others have since extended this work using porcine models, applying rapid rotational accelerations to replicate milder injury patterns observed in human concussion.[19] Finite element modelling of the porcine brain has since shown that rotational acceleration induces diffuse strain in the deep white matter,[20] a region heavily implicated pathologically.[21,22] Together, these studies motivated the need for human measurements to translate findings from animals and establish clinically relevant concussion thresholds.

With the miniaturization of electromechanical systems (MEMS), it became possible to measure head impact kinematics with wearable sensors on humans and move toward developing injury risk functions. Injury risk functions estimate the probability of brain injury from mechanical inputs such as head motion, and are used to establish injury thresholds and evaluate protective equipment performance. Beginning in the early 2000s, the Head Impact Telemetry System (HITS)[23] enabled the first large-scale data collection studies in helmeted sports by embedding accelerometers into American football helmets. Since then, HITS data has informed the Brain Injury Criterion, a rotational velocity-based injury risk function[24] proposed by the National Highway Traffic Safety Administration for automotive crash testing, and the Summation of Tests for the Analysis of Risk (STAR) helmet rating system.[25] HITS used an array of helmet-mounted accelerometers to measure linear acceleration and estimated rotational acceleration using a

centroid-based algorithm.[26] However, it did not capture time-resolved rotational acceleration and was affected by relative motion between the helmet and skull, reducing accuracy.[26,27]

Instrumented mouthguards (iMGs) overcome limitations of motion artifacts by rigidly coupling inertial sensors to the upper dentition, enabling direct six-degree-of-freedom measurements of linear and rotational head kinematics *in vivo*.[28] IMGs have been extensively tested in laboratory and on-field settings,[29–31] and deployed at scale in both helmeted and unhelmeted sports,[32,33] capturing large head impact datasets under real-world conditions. With these data now available, iMG technology enables rigorous testing of the rotational hypothesis for the first time in humans. In the current study, we used a dataset of iMG-measured head impacts to test the long-standing hypothesis that rotational acceleration is a more precise predictor of concussion than linear acceleration. Contrary to the hypothesis, we show that that linear acceleration is a significantly more precise predictor of concussion than rotational acceleration, and propose two risk functions incorporating linear acceleration. We further demonstrate that concussion risk remains substantially high across laboratory impacts during American football helmet testing. Applying the derived risk functions, we show that attenuating linear acceleration with a liquid-pad helmet design can meaningfully reduce predicted concussion risk.

Results

Concussive impacts have larger kinematic and strain magnitudes

We characterized the kinematics and finite-element simulated strains from a dataset that included 3,805 non-concussive impacts and 47 concussive impacts, collected across 203 male and female athletes in American football, Australian football, rugby union, gymnastics, ice hockey, mixed martial arts (MMA) and lacrosse (Supplementary Table 1). Concussive impacts occurred in 40 athletes, with three American football players and one Australian football player sustaining multiple concussions. Loss of consciousness occurred in five Australian football cases, three MMA cases, one collegiate football case, and one youth football case. We calculated peak linear acceleration (**a**), peak rotational acceleration (**α**), peak rotational velocity (**ω**), head impact power (HIP), split into linear and rotational components, and 95th percentile maximum principal strain (MPS95) both globally and regionally.

Figure 1a shows the Stanford MiG2.0, one of the iMG technologies used in this study, and its MEMS sensor components for measuring linear and rotational head impact forces. Figure 1b shows that concussive impacts exhibit significantly greater **a**, **α**, **ω**, and MPS95 compared to non-concussive impacts (*** $p<0.0001$), and that youth concussion magnitudes are much lower than concussion data from older athletes for **a** and **α**. Summary statistics of impact magnitudes are provided in Supplementary Table 2.

Figure 1c shows that the vast majority of impacts fall within a regime where brain deformation is expected to be more sensitive to rotational velocity than to rotational acceleration. This pattern is shown relative to the white reference line, which has a slope equal to the inverse of the brain's natural period (Δt_n), approximately 40 ms when averaged across coronal, sagittal, and axial anatomical planes.[34] This period corresponds to a natural frequency of approximately 25 Hz and represents the duration of one full oscillation of the brain when subjected to dynamic loading. Impacts above this line are indicative of short-duration pulses less than Δt_n, where deformation is primarily influenced by rotational velocity. The predominance of impacts above the brain's natural period suggests that rotational velocity plays a dominant role in brain deformation in this population.

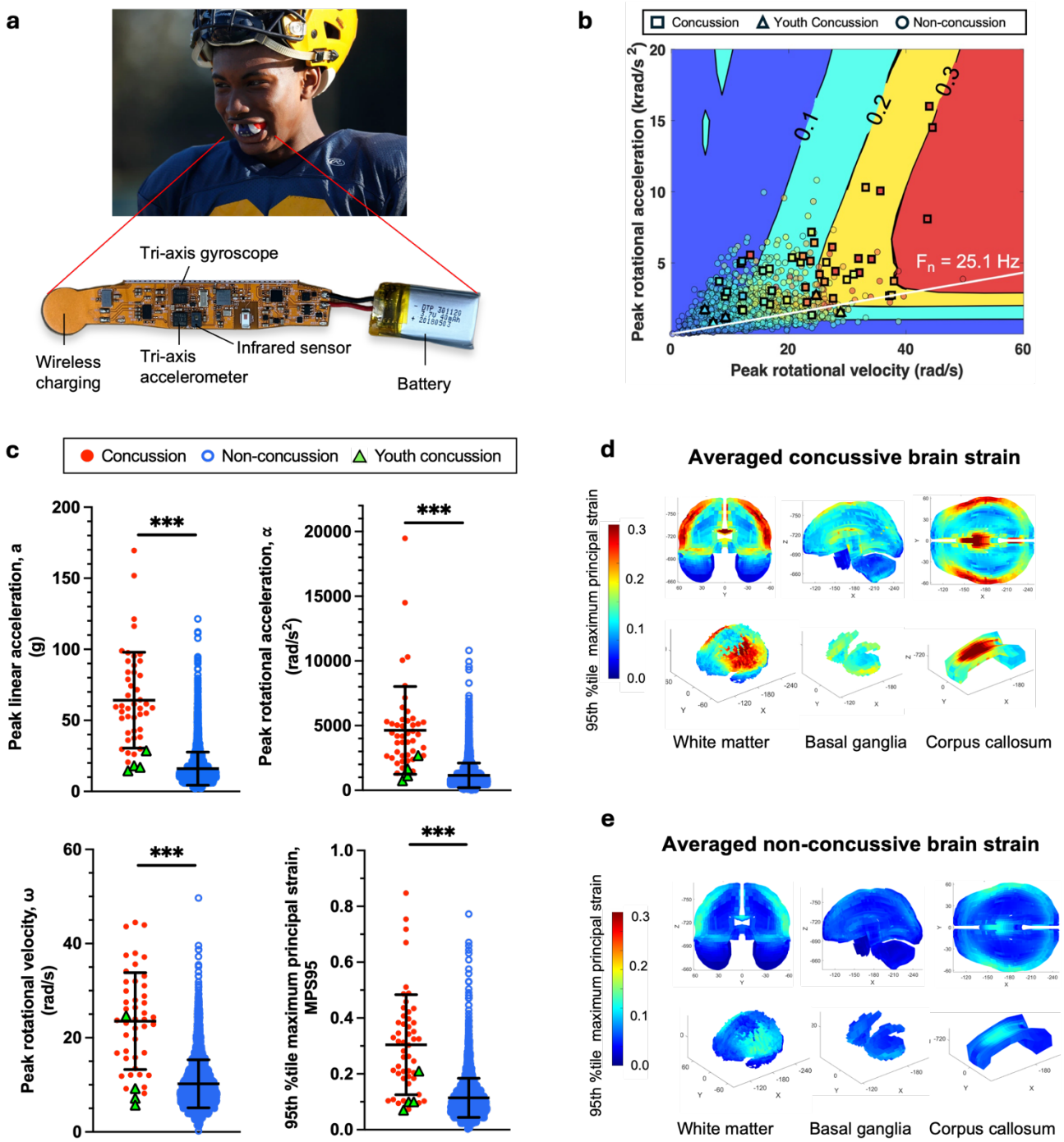

Fig. 1. Differences in kinematics and brain strain between concussive and non-concussive impacts. a, Stanford MiG 2.0 and its sensor board components.[35] b, Distribution of impact magnitudes plotted on a logarithmic scale. Black bars represent the mean and one standard deviation of all impacts in each respective dataset. (***, $p<0.0001$). c, Iso-strain contour plot showing the relationship between peak rotational velocity, peak rotational acceleration, and strain, as predicted by the DAMAGE model.[36] A white reference line is plotted with a slope defined as $\pi/\Delta t_n$, reflecting the brain's estimated natural frequency of 25.1 Hz. Ninety-fifth percentile maximum principal strain patterns averaged across d, concussive and e, non-concussive impacts.

In Figures 1d and 1e, we show differences in brain strain patterns for concussive and non-concussive impacts. Specifically, we show the MPS95 per element averaged across impact types. In concussive impacts, elevated strains are observed in the cortical areas including the upper gray matter (0.36 ± 0.21) and cortical white matter (0.30 ± 0.12), as well as the deep white matter regions such as the basal ganglia (0.28 ± 0.10) and corpus callosum (0.48 ± 0.14). Non-concussive impacts had significantly lower MPS95, ranging from 0.04 to 0.09. (Supplementary Table 3). The distribution of regional strains is shown in Supplementary Figure 2. These findings support Holbourn's original hypothesis that shear deformation underlies brain injury.

In Figure 2, we plot differences in head impact power (HIP), the rate of change of kinetic energy of the head during an acceleration event, split into linear and rotational components. We found that on average, concussive impacts exhibited 7.3 times more linear power than rotational power, while non-concussive impacts had 8.2 times more linear than rotational power. This indicates that linear power, and by extension linear acceleration and velocity, are prominent biomechanical signatures of head impacts in our population.

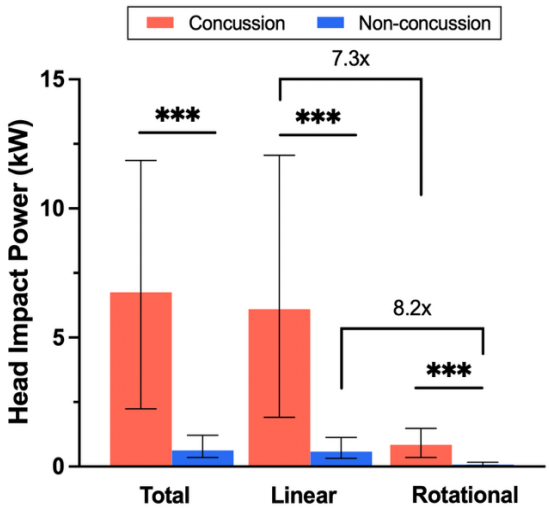

Figure 2. Bar chart comparing head impact power for concussive and non-concussive impacts, split into linear and rotational components. Error bars indicate the interquartile range. In concussive impacts, the mean linear power was 7.3 times greater than the rotational power, while in non-concussive impacts, mean linear power was 8.2 times greater than the rotational power

Linear acceleration is the most precise univariate determinant of concussion

Twelve kinematic and strain-based logistic regression models were developed to assess concussion classification performance and identify candidates for injury risk function development. Model deviance (G^2), Bayesian Information Criterion, LASSO-penalized logistic regression, and dominance analysis were used to screen all candidate predictors. All models had significantly better fit than the null model, but the five models with the best fit were **a**+ **ω**, **a** + **α**, **a**, **α**, and **ω** based on the lowest deviance and Bayesian Information Criterion (Fig. 3a). Additionally, **a**, **ω**, and **α** were consistently the most informative and best-fitting fitting predictors across both LASSO and dominance analyses, based on having the largest R^2 and general dominance scores, respectively (Supplementary Tables 8-9). Therefore, **a** + **ω**, **a** + **α**, **a**, **α**, and **ω** were retained for formal statistical comparison as classifiers and for injury risk function development. This approach both preserved statistical power and enabled testing of our primary hypothesis that rotational acceleration is a more precise predictor of concussion than linear acceleration.

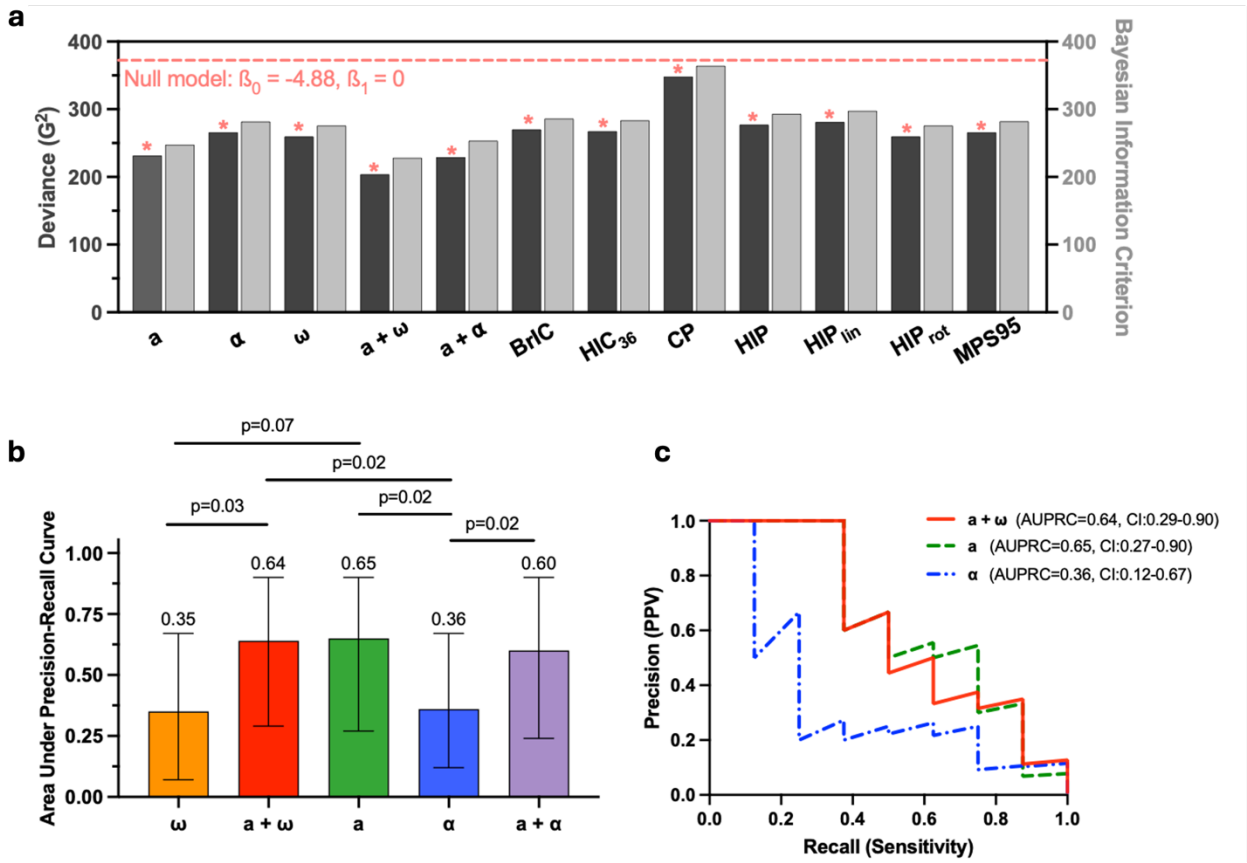

Figure 3. Comparison of model fit and performance for concussion classifiers. Model abbreviations are provided in Supplementary Table 4. **a,** In-sample goodness-of-fit for each model. A lower deviance (G^2) indicates better fit relative to the null model, and all models provided significantly better fit compared to the null model (* $p<0.005$). Bayesian Information Criterion assesses the tradeoff between model fit and complexity, with lower values indicating better performance while penalizing for model complexity. **b**, Area under the precision–recall curve for kinematic models, evaluated on the held-out test set. Black error bars represent 95% confidence intervals. **c**, Precision–recall curves for kinematic classifiers on the held-out test set.

Table 1 summarizes the classification performances on the youth and held-out test sets. No concussions were detected on the youth set. On the held-out set, **a** achieved the highest area under the precision–recall curve (AUPRC, 0.65) and F1 score (0.50). Among univariate models, **a** was followed by **α** (AUPRC=0.36; F1=0.31) and **ω** (AUPRC=0.35; F1=0.30). Differences between **a** and **α** are significant (Figs. 3b-c). Additionally, **a** + **α** (AUPRC=0.60; F1=0.55) offered no detectable improvement over the use of **a** alone. Among bivariate models, **a** + **ω** had the largest AUPRC (AUPRC=0.64, F1=0.40), and significantly outperformed **α** and **ω** (Fig. 3b). It is important to note that the AUPRC of a random classifier, defined as the ratio of positive cases to total cases, is only 0.01, indicating that kinematic metrics alone still provide substantial discriminatory power. Dominance analysis and LASSO further confirmed **a** as the most informative predictor variable, with the highest general dominance score (R^2=0.108) and LASSO coefficient (β=0.91), followed by **ω** (R^2=0.065; β=0.842) and **α** (R^2=0.061; β=0.380).

Model	Peak linear acceleration (**a**)	Peak rotational acceleration (**α**)	Peak rotational velocity (**ω**)	Peak linear acceleration + peak rotational velocity (**a+ ω**)	Peak linear acceleration + peak rotational acceleration (**a + α**)
AUPRC [95% CI][1]	0.65 [0.27, 0.90]	0.36 [0.12, 0.67]	0.35 [0.07, 0.67]	0.64 [0.29, 0.90]	0.60 [0.24, 0.90]
F1 [95% CI][1]	0.50 [0.18, 0.80]	0.31 [0.13, 0.59]	0.30 [0.13, 0.57]	0.4 [0.22, 0.77]	0.55 [0.25, 0.8]
Precision[1]	0.80	0.33	0.33	1.0	0.5
Recall[1]	0.38	0.25	0.25	0.25	0.63
Recall (Youth)[2]	0	0	0	0	0
Decision Threshold[1]	0.2 (78.7 g)	0.1 (5874.2 rad/s^2)	0.1 (29 rad/s)	0.3	0.1

1: Held-out set, 2: Youth set

Table 1. Performance metrics for logistic regression-based injury risk functions. The first test was conducted on the 20% held-out dataset, while recall (sensitivity) was calculated for the dataset containing 4 youth concussions.

Several additional metrics used in automotive and helmet safety assessments were evaluated, including MPS95, Brain Injury Criterion (BrIC),[24] Head Injury Criterion (HIC_{36}),[37] Head Impact Power (HIP),[38] split into linear and rotational components, and Virginia Tech Combined Probability (CP)[39] (Supplementary Table 5). Although linear HIP outperformed rotational HIP based on AUPRC and F1, neither model achieved better fit than the five kinematic models described above. MPS95 and BrIC were among the lowest performers. As a result, these metrics were not used to construct injury risk functions or included in formal statistical comparisons.

Linear acceleration shows a significant association with concussion risk

The five kinematic models identified by best fit were then used to develop injury risk functions. As described above, these included three univariate models (**a**, **ω**, **α**) and two bivariate models (**a** + **α** and **a** + **ω**). Model coefficients are provided in Supplementary Table 6, and the resulting risk functions are shown in Figure 4. The 50% injury risk thresholds were determined to be 100 g for **a**, 8.3 krad/s² for **α** and 40 rad/s for **ω** (Fig. 4a–c).

Next, bivariate models allowed us to assess the relative importance of linear versus rotational terms. In the **a** + **α** model, the 50% risk contour displayed a steep slope, suggesting greater sensitivity to **a**. Consistent with this, odds ratios (OR) indicated **a** was a significant independent predictor of concussion (OR=2.3; 95% CI: 1.5-3.6), while **α** was not (OR=1.3; 95% CI: 0.81-1.9), as its confidence interval included 1. The larger odds ratio for **a** indicates it is a greater risk factor for concussion than **α**. However, the Wald test comparing the two ORs was not statistically significant (Fig. 4f). In the **a** + **ω** model, risk increased comparably with both predictors, as reflected by their similar odds ratios ($OR_{\mathbf{a}}$=2.1; $OR_{\boldsymbol{\omega}}$=2.2) with no significant differences (Fig. 4f).

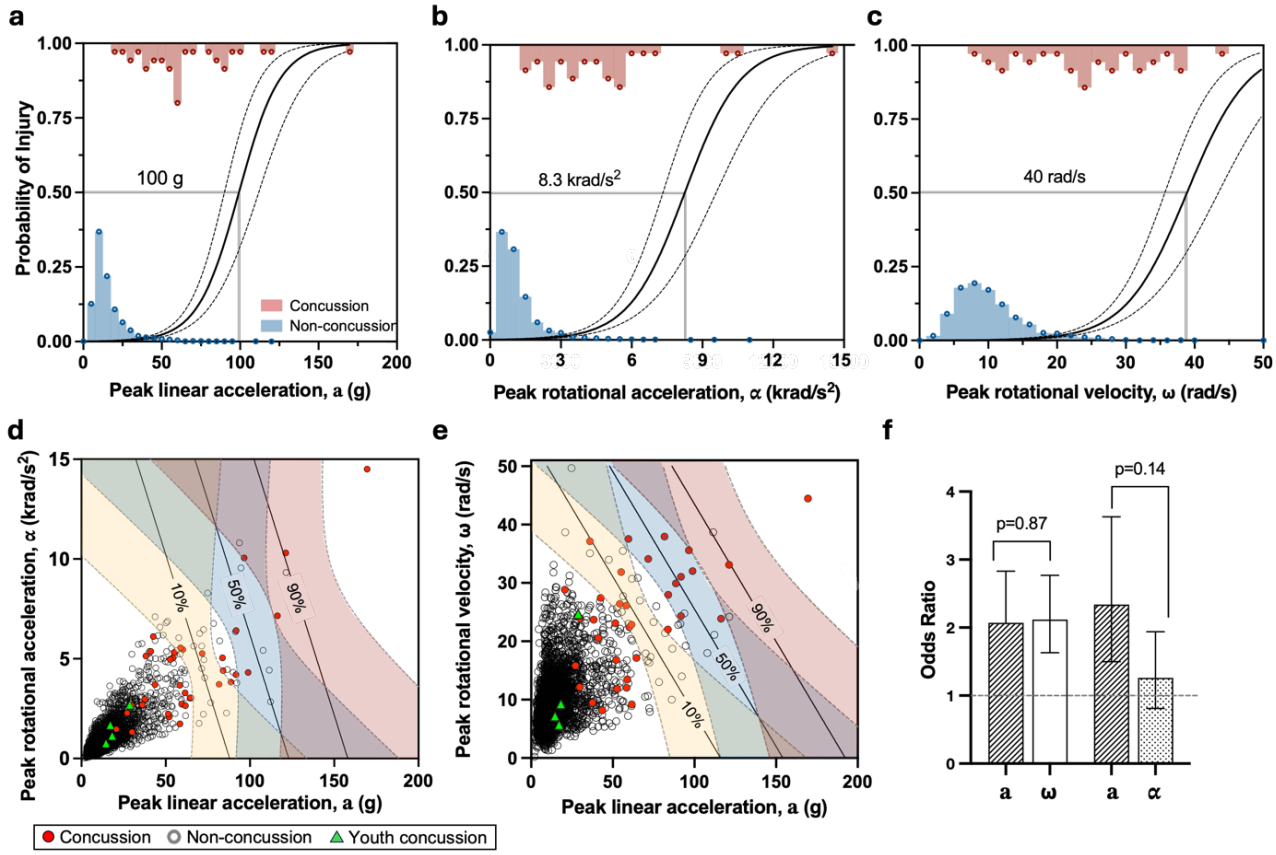

Figure 4. Injury risk functions developed on the 80% training data. Univariate logistic regression models based on a, peak linear acceleration, b, peak rotational acceleration, and c, peak rotational velocity. Solid black lines indicate the fitted logistic regression curves and dashed lines show the 95% confidence intervals. Injury risk functions for d, **a** + **α** and e, **a** + **ω**. The black contours and shaded regions indicate different risk levels and their 95% confidence intervals. Youth concussions are overlaid for comparison and did not contribute to the training data. f, Odds ratios plotted for each predictor in bivariate kinematic models. In the **a** + **α** model, the confidence interval for **α** crosses the reference line at y=1, indicating it is not a significant independent predictor of concussion.

Liquid helmet technology significantly reduces concussion risk

Helmets equipped with novel liquid-filled fit pads were evaluated against a control helmet equipped with stock fit pads using the impact speeds and locations defined in the Virginia Tech Varsity Football Helmet STAR protocol (Fig. 5a-b). Concussion risk was quantified using the derived injury metric $P_{inj}(\mathrm{a} + \omega)$. Across impact velocities, the liquid helmet exhibited consistently lower injury risk compared to the control helmet (Fig. 5c-e). At 3.1 m/s, mean injury risk averaged across impact locations was 1.6% for the Control helmet and 0.8% for the Liquid helmet (Fig. 5c), with statistically significant differences between helmets based on post-hoc comparisons with Šidák correction.

At 4.9 m/s, mean injury risk decreased from 26.7% to 13.4% with the liquid pad, with significant reductions at the back, front, and side locations (Fig. 5d). At the highest impact velocity of 6.4 m/s, the liquid helmet reduced mean injury risk from 73.3% to 55.7%, representing the largest observed reduction in absolute risk, with significant reductions at the back, front, and side locations (Fig. 5e). Peak kinematics and associated risk predictions for individual impacts are provided in Supplementary Table 10.

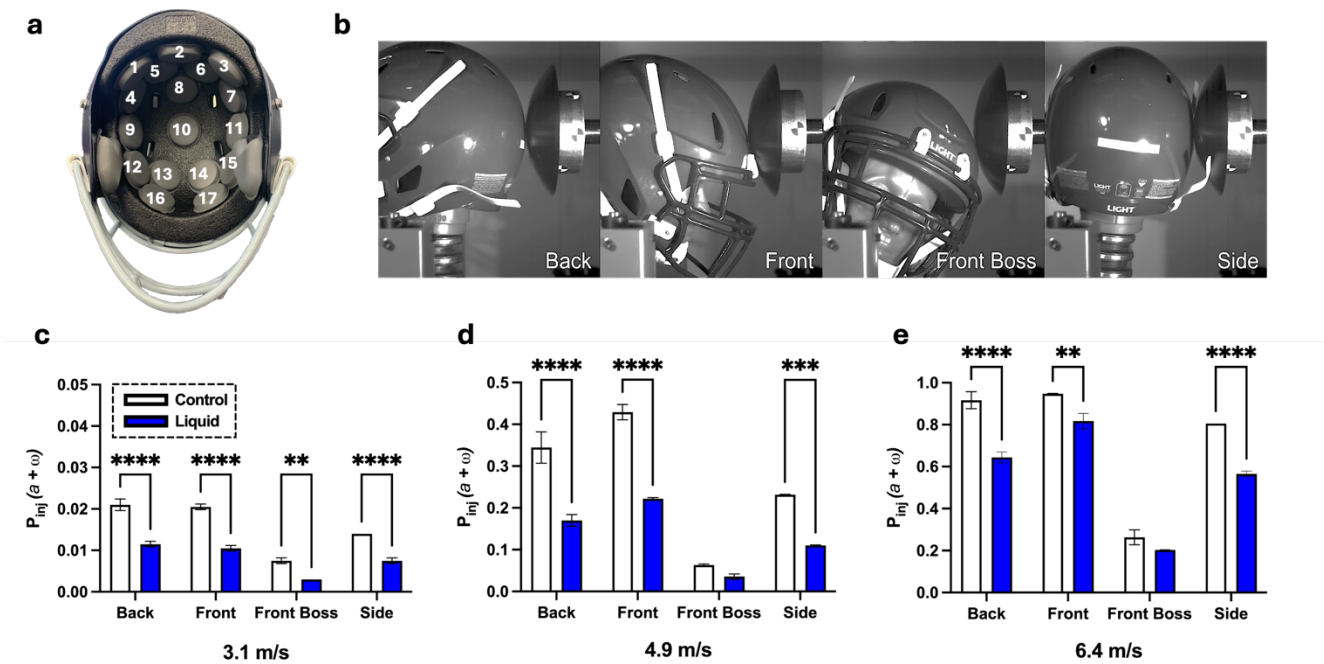

Figure 5. Comparison of helmet technologies for mitigating concussion risk. **a,** Fit pad locations adapted with liquid shock absorbers. **b,** Impact locations tested in the laboratory. **b,** Example of linear acceleration time traces for the 6.4 m/s impact to the back location. Injury risk quantified as $P_{inj}(\mathrm{a} + \omega)$ is shown for helmets equipped with standard fit pads (Control) and liquid fit pads (Liquid) across impacts with velocities of **c**, 3.1 m/s, **d**, 4.9 m/s, and **e**, 6.4 m/s. Bars represent the mean ± standard deviation. Asterisks denote with statistically significant reductions observed at each location (**p < 0.01, **p < 0.001, ***p < 0.0001).

Discussion

The rotational acceleration hypothesis for concussion has guided brain injury prevention research, shaping safety standards and the development of protective equipment. Yet, this hypothesis had not been tested using direct measurements of rotational acceleration during concussion in humans. We addressed this gap by collecting a dataset of directly measured rotational accelerations during human concussions using instrumented mouthguards across multiple sports and age groups. Surprisingly, we found linear acceleration to be a significantly more precise predictor of concussion than rotational acceleration. We developed a new injury risk function using peak linear acceleration and found a 50% concussion risk threshold of 100 g, when filtered at 200Hz. We also developed a bivariate risk function using peak linear acceleration and peak rotational velocity, as both variables were found to be significant independent predictors of concussion. Applying this risk function to football helmet impact tests, we demonstrate that concussion risk can still be meaningfully reduced using liquid-padding technology. Together, these findings indicate that linear acceleration is a primary risk factor for concussion and that it can be substantially reduced to avoid unnecessary brain injury.

Given the utility of single-impact thresholds in helmet and vehicle safety evaluations, we restricted our analysis to the kinematics of the impact linked to each diagnosed concussion and evaluated injury classification and risk using single-event measures. Although repeated head impacts are known to contribute to long-term neurodegenerative disease,[40,41] the extent to which prior exposure modifies instantaneous risk remains debated, and both single-impact and cumulative-impact modeling approaches are ongoing areas of investigation. Prior studies conducted by the National Collegiate Athletic Association and Department of Defense Grand Alliance[42] have shown that injury may be preceded by either a high-magnitude single impact or clusters of lower-magnitude impacts, suggesting that multiple mechanisms may exist for acute concussion.[43] However, safety evaluations typically define pass or fail criteria that are based on individual loading events rather than accumulated exposure, and protective equipment is assessed relative to these thresholds.[39,44–47] As a result, our focus on single-event kinematics is aligned with prevailing safety evaluation practices and the structure of many existing injury risk functions for comparison, and remains an appropriate and widely used framework for estimating acute concussion risk.

Using this single-event modeling approach, we found peak linear acceleration to be a significantly more precise predictor of concussion than peak rotational acceleration. Peak linear acceleration was also the largest risk factor for concussion and the only significant independent contributor in the model that also contained peak rotational acceleration ($\mathbf{a} + \boldsymbol{\alpha}$; Fig. 4d). Peak rotational velocity was also found to be a significant independent risk factor for concussion when evaluated alongside linear acceleration, and the combined model ($\mathbf{a} + \boldsymbol{\omega}$) achieved the second largest AUPRC. Dominance analysis and LASSO-penalized logistic regression further supported the predictive utility of peak linear acceleration as it contributed the most unique and stable predictive signal across both methods, followed by peak rotational velocity. A similar finding was observed in elite men's rugby union using iMGs, where peak linear acceleration was significantly associated with player removal for head injury assessment due to suspected concussion, while peak rotational acceleration was not.[48] However, conclusions from the rugby study are limited by the use of receiver operating characteristic curves for evaluating predictive performance, which does not assess positive predictive value (i.e., precision). In datasets with a low concussion incidence such as the rugby study (58 removals, 5,400 non-removals), the area under the receiver operating

characteristic curve is less informative because it gives equal weight to both classes and can be dominated by correct predictions of the much larger negative class (i.e. impacts without removal from play). In contrast, we used precision–recall, which includes positive predictive value and sensitivity, and offers a more balanced evaluation of the classifier's performance on rare outcomes like concussion.

Likewise, a previous study using HITS football data reported better predictive performance for peak linear acceleration compared to peak rotational acceleration on a dataset of 244 concussions and 62,767 non-concussions.[39] However, to address underreporting, the concussion dataset in the HITS study included non-concussive impacts that were relabeled as concussions based on having large kinematic magnitudes. Additionally, there were no significant differences between peak linear acceleration and peak rotational acceleration in a separate test dataset on professional football impact reconstructions.[39] The HITS study similarly quantified predictive performance using receiver operating characteristic curves, where the area under the curve is driven by the correct classification of the majority negative class of non-concussions. Taken together, these factors complicate the direct interpretation of rotational acceleration as a predictor of clinically diagnosed concussions in the HITs dataset.

An intriguing outcome of the current study is that strain-based and composite injury metrics underperformed simple kinematic measures. We evaluated 95th percentile maximum principal strain (MPS95) and Brain Injury Criterion (BrIC) which are commonly used in research and regulatory settings. MPS95 is the target output of the Diffuse Axonal Multi-Axis General Evaluation (DAMAGE) model, a second-order system for estimating maximum brain strain used in the European New Car Assessment Program safety rating.[47] The National Football League also uses DAMAGE alongside the Head Injury Criterion (HIC_{36}), which is based on linear acceleration, to calculate Helmet Performance Score for helmet safety rankings. Although the Helmet Performance Score has been shown to correlate with on-field concussion incidence,[49] we found that MPS95 had low classification performance compared to kinematic metrics, including HIC_{36} (Supplementary Table 5). Given that HIC_{36} performed well and similarly to peak linear acceleration in our dataset, the observed correlation of Helmet Performance Score with concussion incidence may be driven by its linear acceleration component, $HIC_{36,}$ rather than DAMAGE. Strain prediction models are also dependent on rotational acceleration and rotational velocity inputs, in agreement with Holbourn's hypothesis. We acknowledge that peak rotational acceleration measurements may be subject to higher error rates due to the differentiation of rotational velocity. However, Figure 1b shows that the majority of impacts fall within the loading regime where brain deformation is more sensitive to rotational velocity than rotational acceleration, so it is less plausible that noise in the rotational acceleration input diminished the performance of MPS95. Alternatively, the relatively low performance of MPS95 may reflect limitations in brain model fidelity, as strain-based bicycle helmet rankings have been shown to differ widely across brain models,[50] suggesting our findings may be model-dependent. Regional strain metrics have also been shown to improve classification,[51] though we only evaluated global MPS95 here. BrIC, a rotational velocity-based metric proposed by the National Highway Traffic Safety Association for automotive crash testing, has similarly informed helmet safety evaluations.[46] BrIC had the lowest predictive performance in our analysis (Supplementary Table 5). Prior work has shown that the critical rotational velocity thresholds used in BrIC can be exceeded during voluntary head motions without producing injurious brain strain.[52] This may have led to false positives during classification, which could explain BrIC's relatively lower performance here.

The stronger predictive ability of linear acceleration is a surprising result that may stem from several factors. One possible explanation is that linear power was nearly eight times greater than rotational power across all impacts (Fig. 1b, Supplementary Table 5), indicating that translational motion contributes more to the total mechanical energy transferred to the head. Animal studies[19,20,22,53] have shown that there must be rotational, strain-based, mechanisms of TBI; however, our data suggests that a linear acceleration mechanism for concussion also exists and that it may be prevalent in the population we studied because of the high linear power or other factors.

We speculate one biomechanical mechanism by which linear acceleration could directly contribute to concussion: due to the slightly greater density of the brain compared to the cerebrospinal fluid (CSF), large linear accelerations of the skull may cause differential motion of the brain as it inertially lags behind. At lower linear accelerations, CSF may act as a shock absorber by resisting relative brain motion through inertial flow. However, at higher accelerations, differential brain motion could compress the subarachnoid space and rapidly displace CSF through available outflow pathways such as the foramen magnum, thereby limiting its shock-absorbing capacity and potentially contributing to injury of surrounding structures. We speculate that this displacement might lead to injury due to contact forces between the cortex and the skull, or perhaps at the depths of sulci[41,54,55] as the gyri flex from motion/contact. Alternatively, negative pressure at the contrecoup site could induce cavitation, a phenomenon in which vapor bubbles form and collapse within the CSF, blood, or parenchyma due to rapid pressure changes. Because pressure has shown to correlate strongly with linear acceleration,[15] this mechanism may be relevant in high-acceleration impacts. Cavitation is also a leading hypothesis for TBI from military blast exposure,[56–58] which could support linear acceleration as a unifying theory for blast-related brain injuries and concussion. However, this warrants future investigation as there is limited evidence supporting the occurrence of cavitation *in vivo*. Future studies should investigate brain displacement, pressure gradients, and flow during pure linear acceleration using fluid-structure interaction models.[59,60] Most finite element brain models for head impact treat CSF as a solid and may not capture fluid dynamics, which could be another possible reason why MPS95 had relatively lower predictive ability here. Overall, while we do not dispute that rotational acceleration can cause diffuse brain injury, our findings suggest that alternative or as-yet-unidentified mechanisms may warrant further investigation.

We derived a 50% concussion risk threshold of approximately 100 g (95% CI: 89g−110g) for peak linear acceleration (Fig. 4a). This threshold falls in between prior estimates based on on-field studies. Pellman et al. reported a lower 50% risk level of 85 g based on laboratory reconstructions of 31 impacts (25 concussions, 6 non-concussions) from the National Football League.[45] This could be attributed to the artificially large concussion incidence from selection bias, potentially overestimating the model's ability to distinguish between concussion and non-concussion cases and skewing the risk curve toward lower thresholds. The lower threshold may also reflect methodological limitations of laboratory reconstructions, such as idealized impact conditions and reliance on video resolution for kinematic accuracy. Similarly, McIntosh and colleagues reported a lower 50% risk threshold of 65 g in Australian football using computational multibody reconstructions of 40 impacts (27 concussions, 13 non-concussions),[61] where overrepresentation of concussive cases likely contributed to selection bias and a risk function biased toward lower accelerations. By contrast, HITS data estimated 50% concussion risk at 192 g[25] which is much higher than our observed threshold. This discrepancy may be due to noise introduced by relative motion between the helmet and skull, or the use of a higher filter cutoff frequency (CFC1000),

which could have preserved high-frequency signal or noise components.[26] Additionally, high acceleration false positive impacts due to lack of visual-verification in the non-concussive data could have been present, potentially causing the logistic regression model to learn a decision boundary skewed toward higher magnitudes and shifting estimated risk thresholds upward.

Many safety testing standards permit peak linear accelerations that are much higher than the 50% risk threshold derived in the current study, reflecting historical prioritization for preventing catastrophic head injuries rather than concussion.[13] A recent exception is the Fédération Équestre Internationale proposal to include a 150 g threshold specifically for equestrian helmet concussion testing; however, our model indicates this corresponds to a >99% probability of injury.[62] Based on Virginia Tech laboratory testing of 45 different equestrian helmets, compliance with this proposed standard would result in only 4 helmets (9%) below this 150g threshold.[63] If our model is correct, even these few higher performing helmets would not meaningfully reduce concussion risk. A helmet threshold of 100 g (the 50% risk level with a 200 Hz filter), however, would likely improve safety but requires innovation, which may indeed be possible depending on the energies involved in exposure.

The exposure in football has been better characterized than any other helmet type, so we evaluated the ability of a novel, liquid-filled technology to reduce concussion risk during laboratory football helmet impacts. We characterized risk using the $P_{inj}(\mathbf{a} + \boldsymbol{\omega})$ bivariate function—given its relatively high discriminatory power—and because rotational kinematics were realistically modeled in the laboratory with the inclusion of the neck and sliding torso mass. The helmet equipped with liquid-filled fit pads exhibited significantly lower predicted concussion risk than the control helmet, primarily driven by attenuation of peak linear acceleration (Supplementary Table 10). Across impact velocities, the liquid helmet most consistently reduced risk at the back location, followed by the side, front, and front boss location, which had the fewest significant reductions. Notably, the back and side locations have been identified as common impact sites for concussion,[64,65] and are frequent during helmet-to-ground impacts, which account for 18% of concussions in the National Football League.[66] The improved performance of the liquid helmet is likely due in part to greater compression of the liquid shock absorbers, prototypes of which have been previously shown to enable more stroke to be utilized as the head decelerates.[67] As the shock absorbers compress, fluid is forced through an orifice and pressure builds in proportion to the orifice area and flow rate, the goal of which is to create a regulated resistive force that remains steady throughout the stroke and reduces sharp acceleration spikes.[68–70] The shock-absorbing effect of CSF may protect the brain in a similar manner though this warrants future investigation. CSF may also allow frictionless gliding between the brain and skull during head rotation.[71,72] Reflecting this biological motivation, reducing friction at the head–helmet interface to minimize torque and rotational kinematics has become an important focus of several contemporary concussion mitigation technologies, including slip-liner and deformable liner systems such as MIPS, WaveCel, and SPIN.[73] While these approaches represent progress in addressing rotational components of head motion, our finding that linear acceleration is the most significant predictor of concussion suggests that minimizing force transmission to the head may be at least as important as minimizing torque.

The current dataset included directly measured head kinematics from concussive impacts across children and adult athletes of both sexes. While we did not conduct sex-specific analyses, this remains an important area for future research, particularly given existing evidence that females may be more susceptible to concussion and axonal injury than males.[22,74–76] Our dataset only

included three female concussions from athletes in lacrosse, rugby, and women's artistic gymnastics. Additionally, youth concussions had much lower magnitudes compared to those from older athletes (Supplementary Table 2). The average peak linear acceleration was 19.7 g for youth and 68.3 g for non-youth concussions, while the average peak rotational acceleration was 1,560 rad/s^2 for youth and 4,919 rad/s^2 for non-youth. During testing, the kinematic classifiers could not detect any youth concussions (Table 1), suggesting that much lower thresholds may be needed to accurately assess injury risk in youth athletes and develop effective helmets. Future work is needed to characterize kinematic and strain-based injury thresholds in youth populations using iMGs across a broad range of sports.

This study has several limitations that warrant consideration. First, head impact data were collected using four different iMGs, each validated independently with device-specific filtering and cutoff frequencies. To ensure consistency across devices, kinematic traces were low-pass filtered at 200 Hz. This decision was guided by the fact that half of the dataset came from Prevent iMG data, which were only available with 200-Hz filtering. Further analysis also revealed that adjusting for iMG device and sport in the logistic regression had negligible effects on risk predictions (Supplementary Information). Second, there is some variability in the selection of concussive impacts due to the inclusion of MMA, where concussive impacts were selected based on having the largest peak rotational acceleration prior to diagnosis. Given that our primary finding is that peak linear acceleration is the more precise classifier, this selection approach is unlikely to have biased the results in favor of linear acceleration. Third, there is also a large difference, naturally, between the number of concussive versus non-concussive impacts in this study, which makes classification more challenging. Even so, the 47 concussions reported here represent, to our knowledge, the largest and most diverse iMG-collected concussion dataset assembled to date. Finally, the predictive accuracy of our thresholds and predicted reduction in concussion risk would need to be determined in a prospective study.

Conclusion

To our knowledge, this is the first study to test the rotational acceleration hypothesis on a dataset reflecting true concussion incidence and using directly measured head kinematics. While rotational kinematics have guided concussion prevention due to the brain's susceptibility to shear forces, our findings suggest that linear motion plays a larger role in concussion biomechanics than previously recognized. Across a multi-center dataset of video-verified impacts collected from both male and female athletes, peak linear acceleration was a significantly more precise predictor of concussion than rotational acceleration, and remained a significant independent risk factor for concussion. At the same time, peak rotational velocity remained a significant independent risk factor when considered jointly with linear acceleration, supporting a multivariate description of concussion biomechanics rather than a purely rotational mechanism. We also found a 50% concussion risk threshold of 100 g for peak linear acceleration, lower than any regulatory bodies have considered. Finally, we demonstrated that concussion risk can be meaningfully reduced in laboratory football helmet evaluations using novel liquid-based shock absorption technology. Together, these findings support the feasibility and value of concussion safety evaluations that explicitly account for linear acceleration, alongside rotational kinematics, to better guide helmet design and injury risk reduction.

References and Notes

1. GBD 2017 US Neurological Disorders Collaborators *et al.* Burden of Neurological Disorders Across the US From 1990-2017: A Global Burden of Disease Study. *JAMA Neurol* **78**, 165 (2021).

2. Dewan, M. C. *et al.* Estimating the global incidence of traumatic brain injury. *Journal of Neurosurgery* **130**, 1080–1097 (2019).

3. Blennow, K. *et al.* Traumatic brain injuries. *Nat Rev Dis Primers* **2**, 16084 (2016).

4. Cancelliere, C. *et al.* Systematic Review of Return to Work After Mild Traumatic Brain Injury: Results of the International Collaboration on Mild Traumatic Brain Injury Prognosis. *Archives of Physical Medicine and Rehabilitation* **95**, S201–S209 (2014).

5. Carroll, L. J. *et al.* Systematic Review of the Prognosis After Mild Traumatic Brain Injury in Adults: Cognitive, Psychiatric, and Mortality Outcomes: Results of the International Collaboration on Mild Traumatic Brain Injury Prognosis. *Archives of Physical Medicine and Rehabilitation* **95**, S152–S173 (2014).

6. Cassidy, J. D. *et al.* Systematic Review of Self-Reported Prognosis in Adults After Mild Traumatic Brain Injury: Results of the International Collaboration on Mild Traumatic Brain Injury Prognosis. *Archives of Physical Medicine and Rehabilitation* **95**, S132–S151 (2014).

7. Coronado, V. G. *et al.* Trends in Sports- and Recreation-Related Traumatic Brain Injuries Treated in US Emergency Departments: The National Electronic Injury Surveillance System-All Injury Program (NEISS-AIP) 2001-2012. *Journal of Head Trauma Rehabilitation* **30**, 185–197 (2015).

8. Schiehser, D. M. *et al.* The Relationship Between Postconcussive Symptoms and Quality of Life in Veterans With Mild to Moderate Traumatic Brain Injury. *Journal of Head Trauma Rehabilitation* **30**, E21–E28 (2015).

9. Stein, M. B. *et al.* Risk of Posttraumatic Stress Disorder and Major Depression in Civilian Patients After Mild Traumatic Brain Injury: A TRACK-TBI Study. *JAMA Psychiatry* **76**, 249 (2019).

10. Pietrzak, R. H., Johnson, D. C., Goldstein, M. B., Malley, J. C. & Southwick, S. M. Posttraumatic Stress Disorder Mediates the Relationship Between Mild Traumatic Brain Injury and Health and Psychosocial Functioning in Veterans of Operations Enduring Freedom and Iraqi Freedom. *Journal of Nervous & Mental Disease* **197**, 748–753 (2009).

11. Haagsma, J. A. *et al.* Impact of Depression and Post-Traumatic Stress Disorder on Functional Outcome and Health-Related Quality of Life of Patients with Mild Traumatic Brain Injury. *Journal of Neurotrauma* **32**, 853–862 (2015).

12. Sproule, D. W., Campolettano, E. T. & Rowson, S. Football helmet impact standards in relation to on-field impacts. *Proc Inst Mech Eng P J Sport Eng Technol* **231**, 317–323 (2017).

13. Whyte, T. *et al.* A Review of Impact Testing Methods for Headgear in Sports: Considerations for Improved Prevention of Head Injury Through Research and Standards. *Journal of Biomechanical Engineering* **141**, 070803 (2019).

14. Holbourn, A. H. S. MECHANICS OF HEAD INJURIES. *The Lancet* **242**, 438–441 (1943).

15. Hardy, W. N. *et al.* A Study of the Response of the Human Cadaver Head to Impact. in 2007-22–0002 (2007). doi:10.4271/2007-22-0002.

16. Ommaya, A. K., Hirsch, A. E., Flamm, E. S. & Mahone, R. H. Cerebral Concussion in the Monkey: An Experimental Model. *Science* **153**, 211–212 (1966).

17. Yarnell, P. & Ommaya, A. K. Experimental cerebral concussion in the rhesus monkey. *Bull N Y Acad Med* **45**, 39–45 (1969).

18. Gennarelli, T. A., Thibault, L. E. & Ommaya, A. K. Pathophysiologic Responses to Rotational and Translational Accelerations of the Head. in 720970 (1972). doi:10.4271/720970.

19. Cullen, D. K. *et al.* A Porcine Model of Traumatic Brain Injury via Head Rotational Acceleration. in *Injury Models of the Central Nervous System* (eds Kobeissy, F. H., Dixon, C. E., Hayes, R. L. & Mondello, S.) vol. 1462 289–324 (Springer New York, New York, NY, 2016).

20. Hajiaghamemar, M. & Margulies, S. S. Multi-Scale White Matter Tract Embedded Brain Finite Element Model Predicts the Location of Traumatic Diffuse Axonal Injury. *J Neurotrauma* **38**, 144–157 (2021).

21. Smith, D. H. & Meaney, D. F. Axonal Damage in Traumatic Brain Injury. *Neuroscientist* **6**, 483–495 (2000).

22. Song, H. *et al.* Sex differences in the extent of acute axonal pathologies after experimental concussion. *Acta Neuropathol* **147**, 79 (2024).

23. Rowson, S. *et al.* A Six Degree of Freedom Head Acceleration Measurement Device for Use in Football. *Journal of Applied Biomechanics* **27**, 8–14 (2011).

24. Takhounts, E. G., Craig, M. J., Moorhouse, K., McFadden, J. & Hasija, V. Development of Brain Injury Criteria (BrIC). in 2013-22–0010 (2013). doi:10.4271/2013-22-0010.

25. Rowson, S. & Duma, S. M. Development of the STAR Evaluation System for Football Helmets: Integrating Player Head Impact Exposure and Risk of Concussion. *Ann Biomed Eng* **39**, 2130–2140 (2011).

26. Beckwith, J. G., Greenwald, R. M. & Chu, J. J. Measuring Head Kinematics in Football: Correlation Between the Head Impact Telemetry System and Hybrid III Headform. *Ann Biomed Eng* **40**, 237–248 (2012).

27. O'Connor, K. L., Rowson, S., Duma, S. M. & Broglio, S. P. Head-Impact–Measurement Devices: A Systematic Review. *Journal of Athletic Training* **52**, 206–227 (2017).

28. Rowson, B., Tyson, A., Rowson, S. & Duma, S. Measuring head impacts: accelerometers and other sensors. in *Handbook of Clinical Neurology* vol. 158 235–243 (Elsevier, 2018).

29. Stitt, D., Draper, N., Alexander, K. & Kabaliuk, N. Laboratory Validation of Instrumented Mouthguard for Use in Sport. *Sensors (Basel)* **21**, 6028 (2021).

30. Bartsch, A. J. *et al.* Laboratory and On-field Data Collected by a Head Impact Monitoring Mouthguard. in *2019 41st Annual International Conference of the IEEE Engineering in Medicine and Biology Society (EMBC)* 2068–2072 (IEEE, Berlin, Germany, 2019). doi:10.1109/EMBC.2019.8856907.

31. Liu, Y. *et al.* Validation and Comparison of Instrumented Mouthguards for Measuring Head Kinematics and Assessing Brain Deformation in Football Impacts. *Ann Biomed Eng* **48**, 2580–2598 (2020).

32. Cecchi, N. J. *et al.* Identifying Factors Associated with Head Impact Kinematics and Brain Strain in High School American Football via Instrumented Mouthguards. *Ann Biomed Eng* **49**, 2814–2826 (2021).

33. Evans, L. J. *et al.* Associations Between Instrumented Mouthguard-Measured Head Acceleration Events and Post-Match Biomarkers of Astroglial and Axonal Injury in Male Amateur Australian Football Players. *Sports Med* https://doi.org/10.1007/s40279-024-02138-6 (2024) doi:10.1007/s40279-024-02138-6.

34. Gabler, L. F., Joodaki, H., Crandall, J. R. & Panzer, M. B. Development of a Single-Degree-of-Freedom Mechanical Model for Predicting Strain-Based Brain Injury Responses. *Journal of Biomechanical Engineering* **140**, 031002 (2018).

35. Krieger, L. Concussions: Stanford researchers use high-tech mouth guards to study head trauma in young athletes. *The Mercury News* (2018).

36. Gabler, L. F., Crandall, J. R. & Panzer, M. B. Development of a Second-Order System for Rapid Estimation of Maximum Brain Strain. *Ann Biomed Eng* **47**, 1971–1981 (2019).

37. Newman, J. A. Head Injury Criteria in Automotive Crash Testing. in 801317 (1980). doi:10.4271/801317.

38. Newman, J. A. & Shewchenko, N. A Proposed New Biomechanical Head Injury Assessment Function - the Maximum Power Index. in 2000-01-SC16 (2000). doi:10.4271/2000-01-SC16.

39. Rowson, S. & Duma, S. M. Brain Injury Prediction: Assessing the Combined Probability of Concussion Using Linear and Rotational Head Acceleration. *Ann Biomed Eng* **41**, 873–882 (2013).

40. Daneshvar, D. H. *et al.* Leveraging football accelerometer data to quantify associations between repetitive head impacts and chronic traumatic encephalopathy in males. *Nat Commun* **14**, 3470 (2023).

41. DeMessie, B. *et al.* Soccer Heading Exposure–Dependent Microstructural Injury at Depths of Sulci in Adult Amateur Players. *Neurology* **105**, e214034 (2025).

42. CARE Consortium Investigators *et al.* A National Study on the Effects of Concussion in Collegiate Athletes and US Military Service Academy Members: The NCAA–DoD Concussion Assessment, Research and Education (CARE) Consortium Structure and Methods. *Sports Med* **47**, 1437–1451 (2017).

43. Seifert, J. *et al.* Time Delta Head Impact Frequency: An Analysis on Head Impact Exposure in the Lead Up to a Concussion: Findings from the NCAA-DOD Care Consortium. *Ann Biomed Eng* **50**, 1473–1487 (2022).

44. Kleiven, S. Predictors for Traumatic Brain Injuries Evaluated through Accident Reconstructions. in 2007-22–0003 (2007). doi:10.4271/2007-22-0003.

45. Pellman, E. J., Viano, D. C., Tucker, A. M. & Casson, I. R. Concussion in Professional Football: Location and Direction of Helmet Impacts—Part 2. *Neurosurgery* **53**, 1328–1341 (2003).

46. Baker, C. E. *et al.* How Well Do Popular Bicycle Helmets Protect from Different Types of Head Injury? *Ann Biomed Eng* **52**, 3326–3364 (2024).

47. Ellway, J., Sandner, V., Eggers, A. & Masuda, M. Brain injury calculation. (2022).

48. Allan, D. *et al.* Head Kinematics Associated with Off-Field Head Injury Assessment (HIA1) Events in a Season of English Elite-Level Club Men's and Women's Rugby Union Matches. *Sports Med* https://doi.org/10.1007/s40279-024-02146-6 (2024) doi:10.1007/s40279-024-02146-6.

49. Bailey, A. M. *et al.* Comparison of Laboratory and On-Field Performance of American Football Helmets. *Ann Biomed Eng* **48**, 2531–2541 (2020).

50. Fahlstedt, M. *et al.* Ranking and Rating Bicycle Helmet Safety Performance in Oblique Impacts Using Eight Different Brain Injury Models. *Ann Biomed Eng* **49**, 1097–1109 (2021).

51. Wu, S., Zhao, W., Rowson, B., Rowson, S. & Ji, S. A network-based response feature matrix as a brain injury metric. *Biomech Model Mechanobiol* **19**, 927–942 (2020).

52. Hernandez, F. & Camarillo, D. B. Voluntary Head Rotational Velocity and Implications for Brain Injury Risk Metrics. *Journal of Neurotrauma* **36**, 1125–1135 (2019).

53. Johnson, V. E. *et al.* Mechanical disruption of the blood–brain barrier following experimental concussion. *Acta Neuropathol* **135**, 711–726 (2018).

54. McKee, A. C., Alosco, M. L. & Huber, B. R. Repetitive Head Impacts and Chronic Traumatic Encephalopathy. *Neurosurgery Clinics of North America* **27**, 529–535 (2016).

55. Butler, M. L. M. D. *et al.* Repeated head trauma causes neuron loss and inflammation in young athletes. *Nature* https://doi.org/10.1038/s41586-025-09534-6 (2025) doi:10.1038/s41586-025-09534-6.

56. Moore, D. F. *et al.* Blast Physics and Central Nervous System Injury. *Future Neurol.* **3**, 243–250 (2008).

57. Franck, C. Microcavitation: the key to modeling blast traumatic brain injury? *Concussion* **2**, CNC47 (2017).

58. Panzer, M. B., Myers, B. S., Capehart, B. P. & Bass, C. R. Development of a Finite Element Model for Blast Brain Injury and the Effects of CSF Cavitation. *Ann Biomed Eng* **40**, 1530–1544 (2012).

59. Willinger, R. & Baumgartner, D. Human head tolerance limits to specific injury mechanisms. *International Journal of Crashworthiness* **8**, 605–617 (2003).

60. Zhou, Z., Li, X. & Kleiven, S. Fluid–structure interaction simulation of the brain–skull interface for acute subdural haematoma prediction. *Biomech Model Mechanobiol* **18**, 155–173 (2019).

61. McIntosh, A. S. *et al.* The biomechanics of concussion in unhelmeted football players in Australia: a case–control study. *BMJ Open* **4**, e005078 (2014).

62. *FEI HELMET WORKING GROUP TECHNICAL REPORT - NEW TESTING PROTOCOL*. (2023).

63. Duma, L. A. *et al.* Equestrian STAR: Development of an Experimental Methodology for Assessing the Biomechanical Performance of Equestrian Helmets. *Ann Biomed Eng* **53**, 2309–2332 (2025).

64. Bartsch, A. J. *et al.* High Energy Side and Rear American Football Head Impacts Cause Obvious Performance Decrement on Video. *Ann Biomed Eng* **48**, 2667–2677 (2020).

65. Bailey, A. M. *et al.* Development and Evaluation of a Test Method for Assessing the Performance of American Football Helmets. *Ann Biomed Eng* **48**, 2566–2579 (2020).

66. Lessley, D. J. *et al.* Video Analysis of Reported Concussion Events in the National Football League During the 2015-2016 and 2016-2017 Seasons. *Am J Sports Med* **46**, 3502–3510 (2018).

67. Cecchi, N. J. *et al.* A wearable hydraulic shock absorber with efficient energy dissipation. *International Journal of Mechanical Sciences* **270**, 109097 (2024).

68. Cecchi, N. J., Vahid Alizadeh, H., Liu, Y. & Camarillo, D. B. Finite element evaluation of an American football helmet featuring liquid shock absorbers for protecting against concussive and subconcussive head impacts. *Front. Bioeng. Biotechnol.* **11**, 1160387 (2023).

69. Fanton, M. *et al.* Variable area, constant force shock absorption motivated by traumatic brain injury prevention. *Smart Mater. Struct.* **29**, 085023 (2020).

70. Vahid Alizadeh, H., Fanton, M. & Camarillo, D. B. Collapsible fluid-filled fabric shock absorber with constant force. *Journal of Intelligent Material Systems and Structures* **33**, 590–603 (2022).

71. Zhou, Z., Li, X. & Kleiven, S. Biomechanics of Periventricular Injury. *Journal of Neurotrauma* **37**, 1074–1090 (2020).

72. Ji, S. *et al.* Use of Brain Biomechanical Models for Monitoring Impact Exposure in Contact Sports. *Ann Biomed Eng* **50**, 1389–1408 (2022).

73. Abayazid, F., Ding, K., Zimmerman, K., Stigson, H. & Ghajari, M. A New Assessment of Bicycle Helmets: The Brain Injury Mitigation Effects of New Technologies in Oblique Impacts. *Ann Biomed Eng* **49**, 2716–2733 (2021).

74. Gupte, R. P., Brooks, W. M., Vukas, R. R., Pierce, J. D. & Harris, J. L. Sex Differences in Traumatic Brain Injury: What We Know and What We Sh ould Know. *Journal of Neurotrauma* **36**, 3063–3091 (2019).

75. Hannah, T. C. *et al.* Sex-Related Differences in the Incidence, Severity, and Recovery of Co ncussion in Adolescent Student-Athletes Between 2009 and 2019. *The American Journal of Sports Medicine* **49**, 1929–1937 (2021).

76. McGroarty, N. K., Brown, S. M. & Mulcahey, M. K. Sport-Related Concussion in Female Athletes: A Systematic Review. *Orthopaedic Journal of Sports Medicine* **8**, 2325967120932306 (2020).

77. Camarillo, D. B., Shull, P. B., Mattson, J., Shultz, R. & Garza, D. An Instrumented Mouthguard for Measuring Linear and Angular Head Impact Kinematics in American Football. *Ann Biomed Eng* **41**, 1939–1949 (2013).

78. Rich, A. M. *et al.* Development, Validation and Pilot Field Deployment of a Custom Mouthpiece for Head Impact Measurement. *Ann Biomed Eng* **47**, 2109–2121 (2019).

79. Swenson, A., Miller, L., Urban, J. & Stitzel, J. Head Kinematics by Contact Scenarios in Youth Ice Hockey. *Neurology* **95**, (2020).

80. Tiernan, S. *et al.* Concussion and the severity of head impacts in mixed martial arts. *Proc Inst Mech Eng H* **234**, 1472–1483 (2020).

81. Pritchard, N. S., E. Urban, J., Miller, L. E., Lintner, L. & Stitzel, J. D. AN ANALYSIS OF HEAD KINEMATICS IN WOMEN'S ARTISTIC GYMNASTICS. *SGJ* **12**, 229–242 (2020).

82. Hernandez, F. *et al.* Six Degree-of-Freedom Measurements of Human Mild Traumatic Brain Injury. *Ann Biomed Eng* **43**, 1918–1934 (2015).

83. Aubry, M. *et al.* Summary and Agreement Statement of the First International Conference on Concussion in Sport, Vienna 2001. *The Physician and Sportsmedicine* **30**, 57–63 (2002).

84. Patricios, J. S. *et al.* Consensus statement on concussion in sport: the 6th International Conference on Concussion in Sport–Amsterdam, October 2022. *Br J Sports Med* **57**, 695–711 (2023).

85. O'Brien, W. T. *et al.* Next-Day Serum Glial Fibrillary Acidic Protein Levels to Aid Diagnosis of Sport-Related Concussion. *Neurology* **104**, (2025).

86. Safety Test Instrumentation Stds Comm. Sign Convention for Vehicle Crash Testing. doi:10.4271/J1733_201811.

87. Connor, T. A., Stewart, M., Burek, R. & Gilchrist, M. D. Influence of headform mass and inertia on the response to oblique impacts. *International Journal of Crashworthiness* **24**, 677–698 (2019).

88. Tierney, G. *et al.* Identifying a severity measure for head acceleration events associated with suspected concussions. Preprint at https://doi.org/10.48550/ARXIV.2410.01343 (2024).

89. Lyu, D., Zhou, R., Lin, C., Prasad, P. & Zhang, L. Development and Validation of a New Anisotropic Visco-Hyperelastic Human Head Finite Element Model Capable of Predicting Multiple Brain Injuries. *Front. Bioeng. Biotechnol.* **10**, 831595 (2022).

90. King, G. & Zeng, L. Logistic Regression in Rare Events Data. *Polit. anal.* **9**, 137–163 (2001).

91. Rowson, S., Brolinson, G., Goforth, M., Dietter, D. & Duma, S. Linear and Angular Head Acceleration Measurements in Collegiate Football. *Journal of Biomechanical Engineering* **131**, 061016 (2009).

92. Davis, J. & Goadrich, M. The relationship between Precision-Recall and ROC curves. in *Proceedings of the 23rd international conference on Machine learning - ICML '06* 233–240 (ACM Press, Pittsburgh, Pennsylvania, 2006). doi:10.1145/1143844.1143874.

93. Gabler, L. F., Joodaki, H., Crandall, J. R. & Panzer, M. B. Development of a Single-Degree-of-Freedom Mechanical Model for Predicting Strain-Based Brain Injury Responses. *Journal of Biomechanical Engineering* **140**, 031002 (2018).

94. Domel, A. G. *et al.* A new open-access platform for measuring and sharing mTBI data. *Sci Rep* **11**, 7501 (2021).

Acknowledgements

This work was supported by the Taube Stanford Children's Concussion Initiative, Pac-12 Conference's Student-Athlete Health and Well-Being Initiative, the National Institutes of Health (R24NS098518; K25HD101686; R43NS119134; R44NS119134), the Stanford Maternal and Child Health Research Institute, the Office of Naval Research, and the National Science Foundation Graduate Research Fellowship Program. The authors want to thank Drs. Steven Rowson, Vahidullah Tac, and Xianghao Zhan for providing help with the methodological approach. We Thank Dr. Fady Abayazid for providing feedback on the manuscript. We also thank Drs. Matthew Campbell, Lyndia Wu, Fidel Hernandez, Kaveh Laksari, Michael Fanton, Abigail Swenson, Ty Holcomb, and Madison Marks for data collection efforts. We thank Lauren Evans, Joel Ernest, William Zhou, Che Bonini, Mary-Anne Camenzuli, Luke Boykett, Jason Turner, Av Kumar, and Paul Kennedy for their Australian football data collection efforts. We thank Tie Liang for help with the statistical approach. We thank Abigail Huddleston, Angel Gunaman, and Praveen Sundar for assisting with video review. We thank Kyle Casazza and Quinn Gaughan for their efforts toward laboratory helmet impact testing. J.A.T. acknowledges support from the Stanford Graduate Fellowship, National Science Foundation Graduate Research Fellowship, Enhancing Diversity in Graduate Education Fellowship, and Stanford's Department of Bioengineering.

Author Contributions

D.B.C. and J.A.T. contributed to the conceptualization and initiation of the study. D.B.C., M.M.Z., S.J.M., and J.A.T. contributed to the methodological approach. M.M.Z, G.A.G. and D.B.C. initiated field data collection at Stanford. J.A.T. led the study design and performed all data analyses. S.J.M. oversaw the collection of Australian football data. J.W.H., W.T.O., and S.S.H.R. collected and processed the Australian football data. J.E.U., J.D.S., and N.S.P. contributed Wake Forest concussion data. N.S.P. processed the Wake Forest concussion kinematic data. N.J.C. contributed the laboratory helmet testing data. J.A.T. wrote the manuscript. D.B.C. supervised the analysis and manuscript writing. All authors provided comments on the manuscript.

Competing Interests

D.B. Camarillo and N.J. Cecchi are inventors of and have a financial interest in the liquid shock absorbing technology which is owned by Stanford University and *SoftShox*. D.B. Camarillo is a founder of *SoftShox,* who is currently pursuing a license for this technology from Stanford. All other authors declare no competing interests.

Data Availability

The datasets analyzed during the current study are available from the corresponding author on reasonable request.

Supplementary Materials for

Linear Acceleration Is a Primary Risk Factor for Concussion and a Target for Prevention

Jessica A. Towns[1]*, Nicholas J. Cecchi[1,2], James W. Hickey[3], William T. O'Brien[3], Spencer S.H. Roberts[4], N. Stewart Pritchard[5,6], Jillian E. Urban[5,6], Joel D. Stitzel[5,6], Gerald A. Grant[7], Michael M. Zeineh[8], Stuart J. McDonald[3,9], David B. Camarillo[1,2]

Corresponding author: jtowns03@stanford.edu

The section includes:

Materials and Methods
Supplementary Text
Tables S1 to S10
Figs. S1 to S2
References

Materials & Methods

Mouthguard data was collated among cohorts from American football, Australian football, lacrosse, rugby union, artistic gymnastics, mixed martial arts, and ice hockey, where mouthguard sensors recorded linear and rotational head kinematics. Concussions were diagnosed by trained personnel and confirmed by video review. Video-verified impact kinematics were used to develop injury risk functions and estimate brain tissue-based criteria using finite element analysis. Injury prediction was investigated using univariate and bivariate logistic regression. Finally, a liquid-based helmet technology was shown to reduce concussion risk using the derived bivariate function.

Data description

A total of 3,805 non-concussive and 47 concussive impacts were compiled to construct the dataset for concussion risk modeling and classification (Supplementary Table 1). Concussions were either medically diagnosed or labeled based on visual signs of concussion observed during video review.[64] Kinematic data were collected with custom-fitted instrumented mouthguards, including the Prevent iMG,[64] the In-mouth ADXL/L3G4200D,[77] the Stanford MiG2.0,[31] the HITIQ Smart Mouthguard,[29] and the Wake Forest mouthpiece.[78] The dataset was sourced from youth ice hockey,[79] collegiate women's lacrosse, professional mixed martial arts,[80] collegiate rugby union, women's advanced gymnastics,[81] amateur Australian football, and youth, high-school, and collegiate American football.[64,82] Among concussive impacts, 17 occurred in American football, 19 in Australian football, 5 in mixed martial arts (MMA), 3 in rugby union, 1 in gymnastics, 1 in ice hockey, and 1 in lacrosse. Three concussive impacts involved female athletes in lacrosse, rugby, and gymnastics. Youth was defined as below 14 years of age.

Concussion diagnosis and impact identification

Given the collation of multiple published datasets, concussion diagnosis procedures differed slightly across studies. To ensure consistency, we harmonized concussion identification using two criteria: (1) the presence of visual signs or reported symptoms of injury and (2) visual confirmation of the associated head impact. Importantly, the clinical signs and symptoms used to diagnose concussion are internationally harmonized through successive Concussion in Sport Group consensus statements, which outline a common set of diagnostic indicators across continents and sports, such as disorientation, motor incoordination, balance disturbance, cognitive changes, and athlete-reported symptoms, among many others.[83,84] This global standardization supports the comparability of concussion cases across the American and Australian datasets included in the current study.

In studies with on-site medical staff (youth American football, ice hockey, gymnastics, lacrosse, rugby, Australian football, and Stanford football) concussions were immediately diagnosed by a medical professional based on acute signs, and video review was performed to isolate the associated impact. In the MMA study, post-bout clinical evaluations were performed by a medical professional, which included the neurocognitive SCAT5 assessment. Because multiple strikes occur in rapid succession without opportunities for in-bout medical assessment, the concussive impact was defined as the largest rotational acceleration impact that occurred during the bout. The chosen impact was subsequently verified by video review. Finally, in the Bartsch et al. American football study, both diagnosis and impact identification were performed through retrospective video review for visual signs of concussion.

Australian football, rugby union and lacrosse field data collection

Data collection methods for the published datasets included in our analysis are described in prior work (Supplementary Table 1), while collection methods for unpublished datasets are described here. The Australian football data builds on a 2022 two-team pilot study within the Victorian Amateur Football Association (VAFA) by Evans et al[33] and is primarily drawn from a broader VAFA cohort study investigating blood-based biomarkers of brain injury.[85] A subset of 11 men's teams (186 players) wore HITIQ iMGs over the 2022–2024 seasons to capture impacts exceeding an 8 g threshold. Video verification was conducted using the same procedures,[33] applied to all timestamped concussion cases and a subset of non-concussive impacts from selected matches, based on events passing HITIQ's filtering pipeline; data from verified cases were then reprocessed using a 200 Hz filter. Australian football projects were approved by the Monash University Human Research Ethics Committee (Project IDs: 27684, 36297, 36556) and Deakin University (Project ID: 2022-337).

Additionally, as part of a larger ongoing study, the Prevent iMG was deployed to 21 collegiate rugby players (7 male, 14 female) on the Stanford rugby team to collect data for the complete 2022 season, while the Stanford MiG2.0 was deployed to 11 collegiate women's lacrosse players across 6 practices in the Spring 2018 season. All mouthguards were custom-fitted to the athlete's upper dentition and equipped with a triaxial accelerometer and triaxial gyroscope to record linear accelerations and rotational velocities during head impacts (Fig. 1a). Video footage was recorded at 4k resolution and 60 frames per second for all athlete-exposures using two camera angles to capture both halves of the field. A world clock was filmed at the start of the recording session to enable temporal synchronization between mouthguard-recorded events and session footage. All impacts exceeding a 10g trigger threshold were subject to visual verification, and only video-confirmed impacts were included in our analyses. Data collection was approved by the Stanford University Institutional Review Board (Protocol 45932).

Mouthguard kinematics processing

Kinematics for video-verified impacts measured with the Prevent, HITIQ, Stanford, and In-Mouth iMGs were first transformed to the SAE J211 coordinate system[86] (+X: forward, +Y, to the right, +Z downward). Linear acceleration and rotational velocity were then filtered using a fourth-order Butterworth low pass phaseless filter with a 200 Hz cutoff frequency (-6 dB). Rotational accelerations were next derived from rotational velocity measurements using a five-point stencil derivative and subsequently filtered at 200 Hz. Finally, linear accelerations were transformed to the head's center of gravity using the respective sensor locations for each mouthguard and Equation 1,

$$a^{CG} = a^{MG} + \alpha^{MG} \times \vec{r} + \omega^{MG} \times (\omega^{MG} \times \vec{r}) \quad (1)$$

where a^{CG} is the linear acceleration (m/s^2) at the head's center of gravity for a 50th percentile male, a^{MG} is the linear acceleration of the mouthguard, α is rotational acceleration (rad/s^2), ω is rotational velocity (rad/s), and $\vec{r}$ is the constant distance vector from the accelerometer to the head's center of gravity. The 200 Hz frequency was chosen due to the unavailability of the raw kinematic data measured from the Prevent iMG in the American football dataset, which comprises 47% of our data. The sampling frequency of the iMGs used in this study are large enough such that a 200 Hz frequency cutoff avoids signal aliasing. Methods for evaluating measurement consistency across devices after 200 Hz filtering are provided in the Supplementary Information, and outcomes are

shown in Supplementary Table 8 and Supplementary Figure 1. IMGs specifications are also provided in Supplementary Table 7.

Impacts that were measured by the Wake Forest mouthpiece followed a slightly different approach. First, data were filtered using a fourth-order Butterworth low pass phaseless filter with a 1,650 Hz cutoff frequency (CFC1000) for linear acceleration and a 250 Hz cutoff frequency for rotational velocity. The impact measured from the gymnastics participant was not initially filtered due to the lower 350 Hz sampling rate (Supplementary Table 7). The accelerometer baseline was zero-offset by subtracting the first data point from all subsequent samples. The gyroscope baseline was zero-offset by subtracting the fifth data point from all subsequent samples and setting the preceding 4 samples to zero. Data were then rotated to a conventional coordinate system (+X: forward, +Y, to the left, +Z upward). Rotational acceleration was derived from rotational velocity using the five-point stencil derivative method. Linear acceleration was then transformed to the head's center of gravity using Equation 1. For inclusion in this study, secondary filtering was applied with a 200 Hz cutoff frequency and data were re-rotated to follow the SAEJ211 coordinate system. For all iMGs, peak kinematic values were calculated from the resultant, or Euclidian norm, of the x, y and z directions.

Head impact power (HIP) is defined as the rate at which rotational and translational kinetic energy is transferred to the head, and was calculated using Equation 2,

$$HIP(t) = m \cdot a_x \int a_x dt + m \cdot a_y \int a_y dt + m \cdot a_z \int a_z dt + I_{xx} \cdot \alpha_x \cdot \omega_x + I_{yy} \cdot \alpha_y \cdot \omega_y + I_{zz} \cdot \alpha_z \cdot \omega_z \quad (2)$$

where m is head mass (kg), I_{xx}, I_{yy}, and I_{zz} are the directional components of the head's moment of inertia (kg·cm^2), a is linear acceleration (m/s^2), α is rotational acceleration (rad/s^2), and ω is rotational velocity (rad/s), further split into directional components. We used an average head mass (m) of 4.1 kg and 3.2 kg for male and female athletes, respectively, based on cadaveric data.[87,88] The moments of inertia are described by equations 3-5.[87,88]

$$I_{xx}(kg \cdot cm^2) = 74.8m - 125.5 \quad (3)$$

$$I_{yy}(kg \cdot cm^2) = 72.4m - 90.2 \quad (4)$$

$$I_{zz}(kg \cdot cm^2) = 45.6m - 26.5 \quad (5)$$

Mouthguard data cleaning

All impacts included in this study underwent video verification to ensure impact timestamps aligned with visual events. For mixed martial arts, the concussive impact was defined as the impact with the highest rotational acceleration recorded during the competitive event in which the concussion was diagnosed.[80] This method was used because head impacts occur frequently during competition, making it difficult to isolate a single concussive event when multiple potentially injurious impacts may occur in the same competitive bout. Additionally, one Australian football concussion was excluded since the infrared proximity sensor reading fell below the threshold used to classify true impacts and was therefore considered a false negative. Low proximity readings may reflect decoupling or recoupling between the mouthguard and upper dentition, which can produce noisy fluctuations or unusually low magnitudes relative to the observed head motion.[15] Therefore, this Australian football concussion was not included in the final dataset.

Finite element modeling of head impacts

Maximum principal strains were computed using the Global Human Body Model Consortium 50th percentile male head and brain model (GHBMC M50-H v6.1). Brain tissue responses from the GHBMC model were previously validated with cadaveric data.[89] Mouthguard data were transformed to align with the SAEJ211 coordinate system of the GHBMC model. Linear accelerations were applied to the head's center of gravity and rotational velocities were applied globally. The 95th percentile maximum principal strains (MPS95) were extracted regionally and globally using a custom MATLAB script. Considered brain regions included the corpus callosum, brainstem, midbrain, basal ganglia, cerebral white matter, upper gray matter, lower gray matter, thalamus and cerebellum.

Statistical methods

Kinematics and strain comparisons

All statistical analyses and model development were performed in RStudio (2024.09.0+375). Differences in peak kinematics and MPS95 between concussive and non-concussive impacts were tested using a Wilcoxon Rank Sum test with a Bonferroni correction ($n=7$, $p<0.007$). Additionally, to evaluate consistency across sensor measurements after filtering, empirical cumulative distribution functions of peak linear acceleration, peak rotational velocity, and their primary frequencies were compared between iMGs using a Kolmogorov-Smirnov test (Supplementary Figure 1 and Table 8). Further details on the statistical comparisons are described in the Supplementary Information.

Logistic regression models

We employed logistic regression models in order to 1) quantify how biomechanical metrics relevant to sports and automotive safety classify concussion and 2) derive injury risk functions. We first divided the full dataset into an 80% training set (n=3,078) and 20% held-out test set (n=744) with a fixed random seed and stratified sampling to preserve concussion incidence. Additionally, youth concussions from the Wake Forest cohorts were withheld as a separate test set. All model threshold tuning described below were performed on the training set alone.

On the training set, rare-events logistic models were fit using ReLogit to address small-sample bias inherent in maximum likelihood estimation when the outcome of interest is rare.[90] Twelve candidate models were tested, including peak linear acceleration ($\mathbf{a}$), peak rotational acceleration ($\boldsymbol{\alpha}$), peak rotational velocity ($\boldsymbol{\omega}$), $\mathbf{a} + \boldsymbol{\alpha}$, $\mathbf{a} + \boldsymbol{\omega}$, peak total head impact power (HIP),[38] peak rotational power (HIP_{rot}), peak linear power (HIP_{lin}), Head Injury Criterion (HIC_{36}),[37] Brain Injury Criterion (BrIC),[24] Combined Probability (CP),[39] and 95th percentile maximum principal strain (MPS95). Further justification on the candidate models is described in the Supplementary Information. A prior correction of 5.5 concussions per 1,000 impacts was applied to the intercept term, which is the assumed concussion rate in collegiate American football.[91] This correction reduces bias in baseline probability estimates without affecting the slope coefficients. Models were implemented using the Zelig() function, with standard errors clustered by subject ID to account for within-player correlation. Predictors were standardized to have a mean of 0 and standard deviation of 1. Model fit was assessed by deviance (G^2) and Bayesian Information Criterion.

Classification thresholds were optimized on the training set by sweeping from 0 to 1 in increments of 0.1 to maximize F1. Determined thresholds were then applied to the 20% held-out test set and

performance metrics—including area under the precision–recall curve (AUPRC), F1, precision, and recall—were estimated with 95% confidence intervals using a stratified bootstrap approach over 1,000 iterations. The same thresholds were applied to the held-out youth concussions (n=4) and recall (sensitivity) was calculated.

Injury Risk Functions

To determine which logistic regression models to analyze as injury risk functions and subject to statistical comparison, we performed an initial screening using deviance (G^2), Bayesian Information Criterion, LASSO-penalized logistic regression, and dominance analysis. G^2 and Bayesian Information Criterion were used to assess model fit, while LASSO and dominance analysis evaluated relative predictor importance based on coefficient magnitude and variance explained, respectively. Predictors or models that ranked highly across these approaches were selected for injury risk modeling and statistical comparison. Full methodological details on the LASSO and dominance analyses are provided in the Supplementary Information.

The final subset of features selected for injury risk function development included **a**, **ω**, and **α** based on consistently ranking as the top three predictors across both LASSO regression and dominance analysis. These three features also demonstrated the strongest model fit (G^2 and BIC) relative to other predictor variables. Therefore, univariate injury risk functions included **a**, **ω**, and **α**, and while bivariate functions included linear combinations of **a** and **ω** (Eq. 6) and **a** and **α** (Eq. 7),

$$P_{inj} = \frac{1}{1 + e^{[-(\beta_0 + \beta_1 a + \beta_2 \omega)]}} \tag{6}$$

$$P_{inj} = \frac{1}{1 + e^{[-(\beta_0 + \beta_1 a + \beta_2 \alpha)]}} \tag{7}$$

where **a**, **α**, and **ω** represent peak linear acceleration, peak rotational acceleration, and peak rotational velocity, respectively. Bivariate models were also used to assess the relative contribution of linear and rotational information for injury risk prediction, allowing us to directly test our hypothesis that rotational acceleration is more predictive of concussion than linear acceleration. To do this, odds ratios and their 95% confidence intervals were compared between the linear and rotational term for each bivariate model. Predictor variables were standardized to have a mean of 0 and a standard deviation of 1, enabling comparisons on a common scale. Odds ratios were defined as the exponentiated logistic regression coefficients for a one-standard-deviation increase in each predictor. The Wald Test was used to assess significant differences between odds ratios for bivariate models including a linear and rotational term, with a Bonferroni-adjusted significance level of $p<0.017$. This approach allowed us to determine whether linear or rotational kinematics were more strongly associated with concussion outcome.

Additionally, we tested our hypothesis by comparing AUPRC values on the 20% held-out test set across the five kinematic models: **a**, **α**, **ω**, **a** + **α** (Eq. 6), and **a** + **ω** (Eq. 7). AUPRC differences between models were tested using the pr.test function in the usefun R package, which performs a stratified bootstrap comparison of precision-recall curves based on the Davis and Goadrich formulation.[92] A significance level of $p<0.05$ (two-tailed) was used. AUPRC was chosen due to the highly imbalanced nature of the dataset, as precision-recall more accurately reflects the

model's capability to classify the minority class. Finally, sensitivity was assessed on a second held-out test set of four youth concussions to assess whether decision thresholds derived on adult and young adult data can detect youth injuries.

Laboratory helmet tests

To evaluate whether the proposed concussion risk metric can discriminate differences in helmet impact performance, American football helmets were subjected to controlled laboratory impact tests. Impact testing was conducted using a pneumatic linear impactor and an anthropomorphic test headform. The linear impactor had a ram mass of 15.5 kg and a curved, nylon end cap. The ram struck a size medium NOCSAE headform while it was equipped with a commercially available American football helmet (LS2; LIGHT Helmets; Carlsbad, CA). Following the widely recognized Virginia Tech STAR Helmet Ratings,[25] four impact locations (Back, Front, Front Boss, Side) and three impact speeds (3.1 m/s, 4.9 m/s, 6.4 m/s) were selected for testing (Figure 4).

The helmet model we tested consisted of a composite shell, an expanded polypropylene liner, and 17 energy absorbing fit pads spread throughout its interior (Fig. 5a). Two styles of fit pads were tested in individual helmets that were otherwise identical. The helmet's standard set of fit pads contained D3O (D3O; London, United Kingdom), a non-Newtonian polymer whose stiffness increases with strain rate and which has been widely used in personal protective equipment applications. A modified set of fit pads contained SoftShox technology (SoftShox; Vienna, VA), liquid-based shock absorbers that dissipate impact energy through velocity-dependent fluid flow. This concept has been previously evaluated for American football applications through prototyping and finite element modeling.[67,68] Both styles of fit pads had an identical exterior casing, thus controlling for friction between the headform surface and inner helmet surface, and identical dimensions (diameter = 55 mm, thickness = 18 mm), thus controlling for helmet fit to the headform. Similar to the Virginia Tech STAR protocol, two replicate tests were conducted for each combination of impact location, impact speed, and helmet design, thus totaling 48 impact tests.

Triaxial linear accelerations and angular velocities were collected from the headform's center of gravity by a 6DX PRO sensor (Diversified Technical Systems; Seal Beach, CA) for each test. Linear accelerations and angular velocities were both filtered at 200 Hz. Peak linear accelerations and peak angular velocities were used to compute the bivariate risk function $P_{inj}(\mathbf{a} + \boldsymbol{\omega})$.

Three independent two-way ANOVA's (one at each at impact velocity of 3.1 m/s, 4.9 m/s, and 6.4 m/s) were performed to assess the main effects of helmet technology and impact location, as well as their interaction, on concussive injury risk. When significant effects were identified, post-hoc pairwise comparisons were conducted using Šidák corrections to control the family-wise error rate.

Supplementary Text

Comparison of mouthguard measurement devices

To assess measurement consistency across iMGs after 200 Hz filtering, we computed empirical cumulative distribution functions of peak linear acceleration (**a**), peak rotational velocity (**ω**), and their primary frequencies for impacts recorded by each iMG (Supplementary Figure 1). These metrics were chosen because they are directly measured by the accelerometer(s) and gyroscope contained on each iMG sensor board. To characterize the primary frequency, we first computed the resultant of the triaxial measurements for linear acceleration and rotational velocity using the Euclidean norm. Each resultant trace was demeaned to remove any DC offset. To extract the primary frequency, we computed the discrete Fourier transform (fft in MATLAB) of each demeaned signal to obtain the single-sided amplitude spectrum. The frequency bin with the largest magnitude, excluding the zero-Hz component, was recorded as the primary frequency and used to construct cumulative distribution functions (Supplementary Figure 1c-d). In parallel, we extracted the peak values of the resultant **a** and **ω** time traces and plotted their cumulative distribution functions (Supplementary Figure 1a-b).

To quantitatively assess whether the distributions differed significantly across iMGs, we performed pairwise two-sample Kolmogorov–Smirnov (KS) tests for each metric. These revealed statistically significant differences ($p < 0.05$) in both time- and frequency-domain metrics between several device pairs (Supplementary Table 8). While KS tests can detect differences in measurement distributions, they do not necessarily indicate that these differences meaningfully alter injury risk predictions. To evaluate this, we constructed univariate Bayesian logistic regression models for **a** and **ω**, including random intercepts for mouthguard type and sport, as well as an offset to account for the rare incidence of concussion (5.5 concussions per 1000 impacts).[39] We compared predicted concussion probabilities from these models to those from our prior models that did not include random effects. The correlation between predicted risks from the paired models was extremely high (Supplementary Figure 1), suggesting that despite distributional differences between devices, the influence on estimated concussion risk was negligible.

Brain sensitivity to rotational velocity and rotational acceleration

To evaluate whether brain strains in our dataset were more sensitive to peak rotational velocity (**ω**) or peak rotational acceleration (**α**), we plotted DAMAGE[36] (equivalent to MPS95) as a function of both **ω** and **α** and examined where human impacts fell relative to a fixed slope representing the brain's natural frequency (Supplementary Figure 3). First, we defined a two-dimensional grid of peak rotational velocities (**ω**: 0.1–100 rad/s) and peak rotational accelerations (**α**: 1–20,000 rad/s²) spanning the full range of head impacts in our dataset. For each (**ω**, **α**) pair, a half-sine rotational-acceleration pulse was constructed at 1 ms resolution over a 2 s window, and used as input to the DAMAGE model. The resulting triplets [**ω**, **α**, DAMAGE] formed a simulation-only design matrix. To create continuous contour surfaces, these discrete DAMAGE values were interpolated onto a regular (**ω**,**α**) mesh using MATLAB's griddata function with a natural neighbor scheme. Next, we computed DAMAGE for the 3,852 human impacts in our dataset and overlaid them on the interpolated contours. Finally, to demarcate the kinematic boundary where **ω** and **α** contributions to brain strain are equal, we overlaid a straight reference line whose slope is directly proportional to the brain's natural frequency (f_n) using Equation 1,

$$\alpha = \pi f_n \omega \quad (1)$$

where f_n was estimated to be 25.1 Hz across the coronal, sagittal, and axial anatomical planes.[93]

Candidate models for classification and injury risk function development

We evaluated twelve logistic regression models to compare the predictive value of linear, rotational, and strain-based metrics for concussion classification and injury risk modeling. These models were selected based on their prevalence in head injury biomechanics research and safety standards. To prioritize which models were included in injury risk function development and comparative statistical testing, we applied multiple screening approaches including deviance, Bayesian Information Criterion, LASSO-penalized logistic regression, and dominance analysis.

Deviance and Bayesian Information Criterion assessed model fit across the twelve candidates. LASSO and dominance analysis were conducted using the ten unique predictors represented in these models (Supplementary Table 9). LASSO was performed using the glmnet R package with a binomial family and 5-fold cross-validation to identify the optimal penalty parameter, lambda. The L1 regularization penalty constrains the sum of the absolute values of the coefficients (n=10 coefficients) to be less than or equal to the specified constant determined by lambda, encouraging sparsity. Predictors were standardized prior to fitting. Dominance analysis was conducted on a full logistic regression model (n=10 predictors) using the dominanceanalysis R package. General dominance scores were computed using McFadden's pseudo-R^2 to quantify each predictor's average contribution across all possible subset models.

LASSO and dominance analysis also complemented our other statistical approaches. For instance, odds ratios quantified the direction and strength of each predictor's independent association with injury risk; area under the precision−recall curve measured the classification performance of each model in the context of class imbalance; LASSO identified relative predictor importance under regularized logistic regression; and dominance analysis estimated each predictor's average contribution to model fit. Across these approaches, **a**, followed by **ω** and **α** consistently ranked among the most important and best-fitting predictor variables. As a result, we focused injury risk function development on models containing these three predictors. This prioritization ensured that the resulting injury risk functions were both well-fitting and practically useful, and reduced the number of formal statistical comparisons needed, thereby preserving statistical power on our limited concussion dataset. Other potential predictors, such as region-specific brain strains or directional kinematics, were excluded due to limited sample size of the concussions. We also excluded peak linear velocity, as it is not a widely used injury metric in safety standards or head injury research.

Authors	Sport	Level(s)	Gender(s)	Measurement Device	No. Concussions	No. Non-concussions	Diagnostic criteria
Current study	Lacrosse	Collegiate	Female	Stanford MiG2.0	1	102	Immediate diagnosis
Current study	Rugby	Collegiate	Female/ Male	Prevent iMG	3	469	Immediate diagnosis/ player identification of impact
Domel et al.[94]	American football	Collegiate	Male	Stanford MiG2.0	0	359	
Hernandez et al.[82]	American football	Collegiate	Male	In-Mouth (ADXL377/ L3G4200D)	1	0	Immediate diagnosis
Bartsch et al.[64]	American football	High-school, collegiate	Male	Prevent iMG	13	1782	Visual signs of concussion
Tiernan et al.[80]	Mixed martial arts	Professional, semi-professional, amateur	Male	Stanford MiG 2.0	5	304	Largest acceleration impact immediately prior to diagnosis
Evans et al.[33] and ongoing study	Australian football	Amateur	Male	HITIQ	19	776	Immediate diagnosis
NIH Grant K25HD101 686	American football	Youth	Male	WF	3	0	Immediate diagnosis
Pritchard et al.[81]	Gymnastics	Advanced	Female	WF	1	0	Immediate diagnosis
Swenson et al.[79]	Ice hockey	Youth	Male	WF	1	0	Immediate diagnosis

Supplementary Table 1. Head impact datasets used in this study.

	Concussion								Non-concussion*			
	Mean		*Median*		*95th%*		*SD*		*Mean*	*Median*	*95th%*	*SD*
	Non-Youth	*Youth*	*Non-Youth*	*Youth*	*Non-Youth*	*Youth*	*Non-Youth*	*Youth*				
PLA (g)	68.3	19.7	60.2	17.6	120.7	27.2	32.2	6.2	16.0	12.6	39.0	11.7
PRA (rad/s^2)	4919	1560	4315	1399	10281	2536	3402	841	1156	899	2941	956
PRV (rad/s)	24.6	11.7	23.9	8.2	43.1	22.4	9.8	8.8	10.2	9.2	20.3	5.1
HIP_{total} (kW)	10	0.78	8.4	0.79	31.7	1.1	8.9	0.33	1.0	0.6	3.7	1.7
HIP_{lin}(kW)	9.5	0.67	8.1	0.76	27.5	0.82	8.6	0.22	1.0	0.5	3.5	1.6
HIP_{rot}(kW)	1.5	0.26	1.1	0.09	4.7	0.7	1.8	0.37	0.1	0.1	0.4	0.2

**Non-concussive impacts do not include youth data.*

Supplementary Table 2. Kinematics summary statistics for concussive and non-concussive impacts.

	Concussion				Non-concussion			
	Mean	*Median*	*95th%*	*SD*	*Mean*	*Median*	*95th%*	*SD*
Global	0.32	0.32	0.70	0.18	0.12	0.11	0.26	0.07
White matter	0.30	0.30	0.65	0.17	0.12	0.10	0.26	0.07
Upper gray matter	0.36	0.35	0.80	0.21	0.14	0.12	0.29	0.08
Lower gray matter	0.20	0.20	0.39	0.11	0.08	0.07	0.16	0.04
Thalamus	0.27	0.24	0.56	0.20	0.08	0.07	0.18	0.06
Brainstem	0.23	0.21	0.44	0.16	0.06	0.15	0.04	0.08
Corpus callosum	0.48	0.36	1.28	0.41	0.11	0.08	0.27	0.10
Basal ganglia	0.28	0.26	0.54	0.16	0.10	0.09	0.22	0.06
Cerebellum	0.13	0.13	0.21	0.07	0.04	0.04	0.09	0.02

Supplementary Table 3. Regional strain summary statistics for concussive and non-concussive impacts.

Metric	Abbreviation
Peak linear acceleration	**a**
Peak rotational velocity	**ω**
Peak rotational acceleration	**α**
95th percentile maximum principal strain	MPS95 (%)
Head injury criterion[37]	HIC_{36}
Brain injury criterion[24]	BrIC
Combined probability[39]	CP
Head impact power[38]	HIP (kW)
Linear head impact power	HIP_{lin} (kW)
Rotational head impact power	HIP_{rot} (kW)

Supplementary Table 4. Kinematic and strain-based model abbreviations referenced in this study.

Metric	AUPRC	F1	Precision	Recall
MPS95	0.28	0.29	0.33	0.25
HIP	0.51	0.50	0.75	0.38
HIP_{lin}	0.51	0.50	0.75	0.38
HIP_{rot}	0.39	0.35	0.50	0.25
HIC_{36}	0.60	0.36	0.66	0.25
BrIC	0.18	0.25	0.22	0.25
CP	0.45	0.36	0.67	0.25

Supplementary Table 5. Performance metrics for additional kinematic- and strain-based classifiers.

Model	Intercept	B1	B2
Peak linear acceleration	-7.547	7.610×10^{-2}	-
Peak rotational acceleration	-7.018	8.502×10^{-4}	-
Peak rotational velocity	-8.677	2.232×10^{-1}	-
Peak linear acceleration + peak rotational velocity	-9.116	5.509×10^{-2}	1.415×10^{-1}
Peak linear acceleration + peak rotational acceleration	-7.620	6.347×10^{-2}	2.111×10^{-4}

Supplementary Table 6. Coefficients for injury risk functions.

	In-mouth (ADXL377/ L3G4200D)	Stanford MiG2.0	Prevent iMG	HITIQ Nexus	Wake Forest Mouthpiece
Sampling rate (Accel)	1024 Hz	1000 Hz	3200 Hz	3200 Hz	350[a] , 4684[b], & 6400[c] Hz
Sampling rate (Gyro)	1024 Hz	8000 Hz	3200 Hz	800 Hz	350[a], 1565 [b], & 6400[c] Hz
Measurement range (Accel)	± 200 g (1 tri-axis)	± 400 g (1 tri-axis)	± 200 g (1 tri-axis)	± 200 g (3 tri-axis)	± 200g (1 tri-axis)
Measurement range (Gyro)	± 40 rad/s (1 tri-axis)	± 70 rad/s (1 tri-axis)	± 35 rad/s (1 tri-axis)	± 35 rad/s (1 tri-axis)	± 35[a,c] rad/s ± 40[b] rad/s (1 tri-axis)
Output time window	100 [-25, 75] ms	200 [-49, 150] ms	50 [0, 50] ms	100 [-20, 80] ms	60 [-15, 45] ms
Triggering sensor	Accel.	Accel.	Accel.	Accel.	Accel.
Triggering threshold	10 G	10 G	5 G	8 G	5 G
No. measured impacts	1	771	2280	795	5

a: Gymnastics, b: ice hockey, c: American football

Supplementary Table 7. Specifications for instrumented mouthguards used in this study.

Mouthguard 1	Mouthguard 2	P value			
		a (g)	**a** (Hz)	**ω** (rad/s)	**ω** (Hz)
HITIQ	Stanford MiG	3.42×10^{-23}	1.33×10^{-318}	0.020	2.45×10^{-245}
HITIQ	Prevent	9.78×10^{-6}	8.39×10^{-223}	0.002	0
HITIQ	Wake Forest	0.00713	0.00144	0.464	5.61×10^{-4}
Stanford MiG	Prevent	1.48×10^{-18}	0	0.922	0
Stanford MiG	Wake Forest	0.00940	2.80×10^{-5}	0.359	1.85×10^{-3}
Prevent	Wake Forest	0.00905	7.01×10^{-4}	0.374	1.93×10^{-5}

Supplementary Table 8. Results of Kolmogorov Smirnov test to compare the distributions of measured kinematics between mouthguard devices. Distributions for measured peak linear acceleration (g), peak rotational velocity (rad/s), and their primary frequencies (Hz) were compared.

Predictor	General Dominance (McFadden R^2)	LASSO Coefficient (standardized)
a	0.108	0.912
ω	0.065	0.842
α	0.061	0.380
HIC36	0.051	–0.097
MPS95	0.050	0.206
HIP_{rot}	0.046	–0.005
BrIC	0.046	–0.362
HIP	0.042	0.000
HIP_{lin}	0.041	0.000
CP	0.029	–0.242

Supplementary Table 9. Results from LASSO-penalized logistic regression and dominance analysis for unique predictors screened for injury risk function development.

Helmet	Impact Location	Velocity (m/s)	Peak linear acceleration, a (g)	Peak rotational acceleration, α (rad/s²)	Peak rotational velocity, ω (rad/s)	$P_{inj}(\mathbf{a} + \boldsymbol{\omega})$
Control	Back	3.1	50.7 ± 0.9	2187 ± 66	17.6 ± 0.1	0.021 ± 0.000
Control	Back	4.9	83.2 ± 2.6	3495 ± 116	27.5 ± 0.2	0.345 ± 0.040
Control	Back	6.4	110 ± 1	4715 ± 118	39.0 ± 3.5	0.917 ± 0.040
Control	Front	3.1	47.5 ± 0.0	1964 ± 23	18.7 ± 0.2	0.0205 ± 0.000
Control	Front	4.9	76.0 ± 0.1	3326 ± 132	32.9 ± 0.5	0.429 ± 0.020
Control	Front	6.4	103 ± 1	4838 ± 30	44.7 ± 0.2	0.947 ± 0.000
Control	Front Boss	3.1	38.2 ± 0.1	3236 ± 128	15.2 ± 0.4	0.00750 ± 0.000
Control	Front Boss	4.9	58.2 ± 0.0	4358 ± 108	22.7 ± 0.3	0.0630 ± 0.000
Control	Front Boss	6.4	73.7 ± 2.0	5337 ± 313	28.5 ± 0.5	0.263 ± 0.040
Control	Side	3.1	37.0 ± 0.2	3436 ± 2	19.9 ± 0.0	0.0140 ± 0.000
Control	Side	4.9	64.2 ± 0.1	5301 ± 51	31.0 ± 0.1	0.232 ± 0.000
Control	Side	6.4	90.8 ± 0.3	7011 ± 14	39.1 ± 0.1	0.805 ± 0.000
Liquid	Back	3.1	40.1 ± 0.9	1737 ± 3	17.3 ± 0.1	0.0115 ± 0.000****
Liquid	Back	4.9	68.0 ± 1.3	2846 ± 74	26.8 ± 0.2	0.170 ± 0.010****
Liquid	Back	6.4	92.5 ± 1.5	4060 ± 83	32.7 ± 0.2	0.644 ± 0.030****
Liquid	Front	3.1	34.1 ± 1.1	1432 ± 52	19.0 ± 0.1	0.0105 ± 0.000****
Liquid	Front	4.9	60.3 ± 0.1	3186 ± 1	32.1 ± 0.1	0.222 ± 0.000****
Liquid	Front	6.4	86.4 ± 3.0	4630 ± 116	41.4 ± 0.6	0.817 ± 0.040**
Liquid	Front Boss	3.1	28.2 ± 0.1	1779 ± 38	13.2 ± 0.0	0.00300 ± 0.000**
Liquid	Front Boss	4.9	49.1 ± 2.1	3011 ± 123	21.9 ± 0.4	0.0355 ± 0.010
Liquid	Front Boss	6.4	65.2 ± 0.8	4205 ± 184	29.4 ± 0.2	0.203 ± 0.000
Liquid	Side	3.1	31.0 ± 1.1	2290 ± 94	17.8 ± 0.6	0.00750 ± 0.000****
Liquid	Side	4.9	54.1 ± 0.1	4392 ± 105	28.6 ± 0.1	0.110 ± 0.000***
Liquid	Side	6.4	77.0 ± 1.1	6156 ± 133	36.4 ± 0.1	0.566 ± 0.010****

Supplementary Table 10. Results from laboratory helmet impacts. Values represent the mean ± standard deviation. Asterisks denote statistically significant reductions in concussion risk compared to the Control helmet based on post-hoc comparisons with Šidák correction (**p < 0.01, **p < 0.001, ***p < 0.0001).

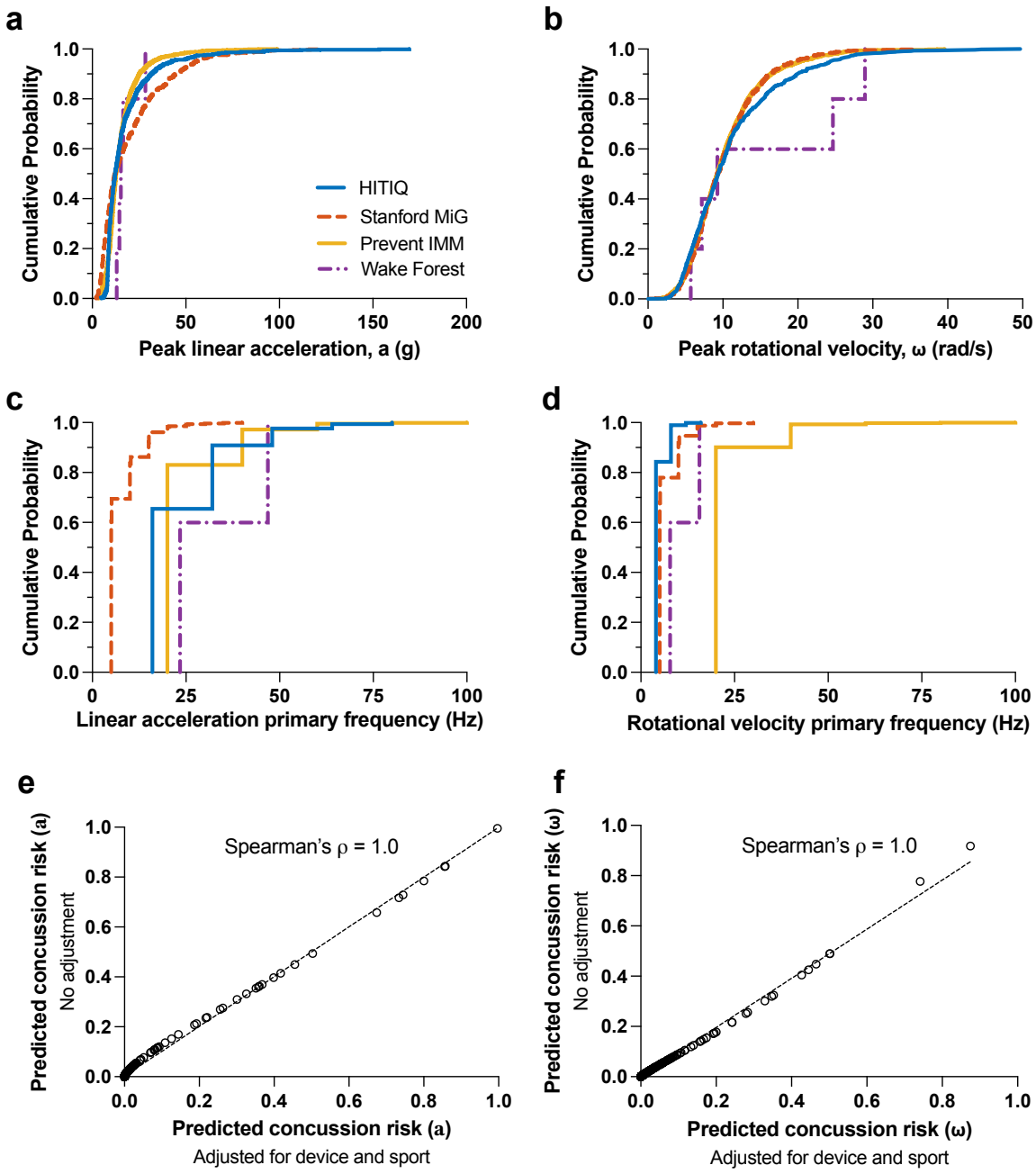

Supplementary Figure 1. Empirical cumulative distribution functions comparing peak kinematic measurements in the time and frequency domains across datasets with different mouthguard devices. **a,** Peak linear acceleration and **b,** peak rotational velocity distributions for each iMG. Distribution of primary frequencies for **c**, peak linear acceleration and **d**, peak rotational velocity. We note that HITIQ data reflect raw signals reprocessed using a 200 Hz low-pass filter, not the manufacturer's default output. **e-f,** Comparison of concussion risk predicted with and without adjusting the logistic regression model for mouthguard device type and sport using **e**, peak linear acceleration and **f**, peak rotational velocity. Despite measurable differences in kinematic distributions across mouthguard devices, adjusting for device and sport had minimal influence on predicted risk.

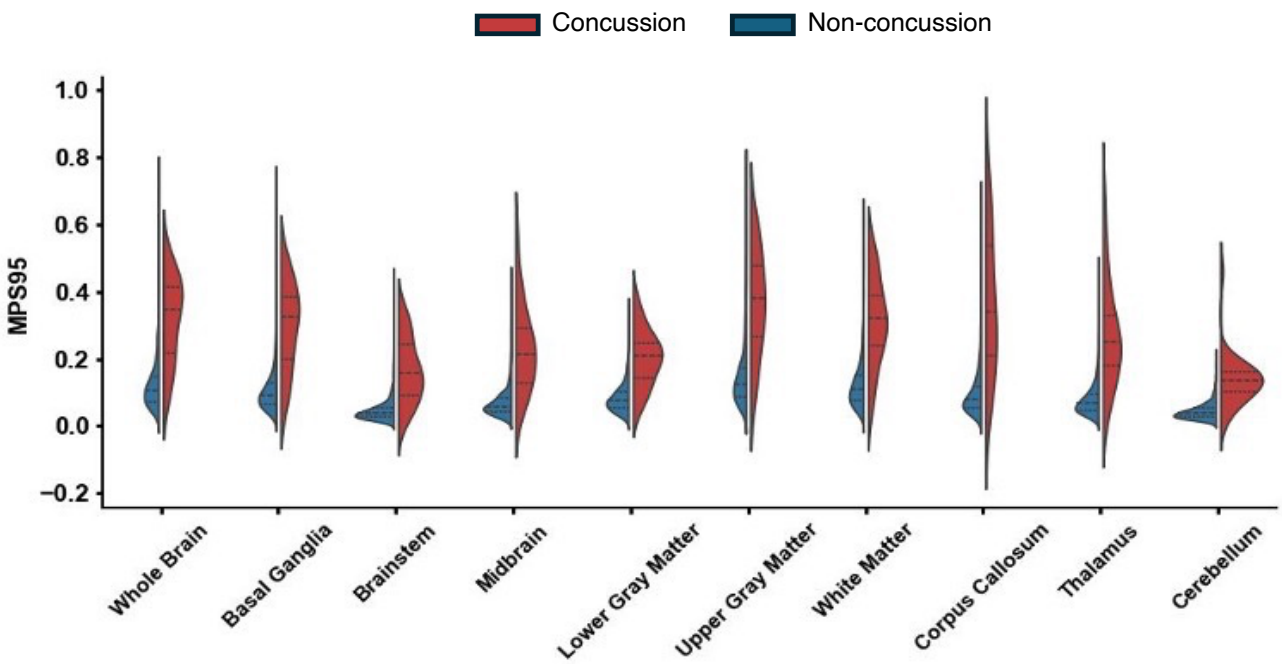

Supplementary Figure 2. Distribution of regional MPS95. Points are plotted per-player per-region. Dashed lines represent the median and interquartile range.